Incisor enamel microstructure of West Indian caviomorph hystricognathous rodents (Octodontoidea and Chinchilloidea)

Laurent Marivaux, Lázaro W Viñola López, Myriam Boivin, Léa da Cunha, Pierre- Henri Fabre, Renaud Joannes-Boyau, Gilles Maincent, Philippe Münch, Narla S Stutz, Jorge Vélez-Juarbe, et al.

Journal of Mammalian Evolution (Doi: https://doi.org/10.1007/s10914-022-09631-7)

Incisor enamel microstructure of West Indian caviomorph hystricognathous rodents (Octodontoidea and Chinchilloidea)

Laurent Marivaux[1,*], Lázaro W. Viñola López[2], Myriam Boivin[3], Léa Da Cunha[1], Pierre-Henri Fabre[1,4], Renaud Joannes-Boyau[5], Gilles Maincent[6], Philippe Münch[7], Narla S. Stutz[1,8], Jorge Vélez-Juarbe[9] and Pierre-Olivier Antoine[1]

[1] Laboratoire de Paléontologie, Institut des Sciences de l'Évolution de Montpellier, Univ Montpellier, CNRS, IRD, cc64, Place Eugène Bataillon, F-34095 Montpellier Cedex 05, France

[2] Florida Museum of Natural History, University of Florida, Gainesville, FL 32611-7800, USA

[3] Laboratorio de Paleontología de Vertebrados, Instituto de Ecorregiones Andinas (INECOA), Universidad Nacional de Jujuy, CONICET, IdGyM, Av. Bolivia 1661, San Salvador de Jujuy 4600, Jujuy, Argentina

[4] Mammal Section, Life Sciences, Vertebrate Division, The Natural History Museum, Cromwell Rd., South Kensington, London SW7 5BD, UK

[5] Geoarchaeology and Archaeometry Research Group (GARG), Southern Cross GeoScience, Lismore Campus, 1 Military Rd., East Lismore, NSW, 2480, Australia

[6] Devé, F-97133 Saint-Barthélemy, French West Indies

[7] Géosciences Montpellier (UMR 5243, CNRS/UM/Université des Antilles), c.c. 060, Université de Montpellier (UM), Place Eugène Bataillon, F-34095 Montpellier Cedex 05, France

[8] Programa de Pós-Graduação em Geociências, Universidade Federal do Rio Grande do Sul, Av. Bento Gonçalves, 9500, 91501-970 Porto Alegre, Brazil

[9] Department of Mammalogy, Natural History Museum of Los Angeles County, 900 Exposition Boulevard, Los Angeles, CA 90007, USA

*** Corresponding author:** Laurent Marivaux

Laboratoire de Paléontologie, c.c. 064

Institut des Sciences de l'Évolution de Montpellier

(ISE-M, UMR 5554 CNRS/UM/IRD)

Université de Montpellier

Place Eugène Bataillon

F-34095 MONTPELLIER Cedex 05

Phone: +33 467 144 911

E-Mail: Laurent.Marivaux@UMontpellier.fr

ORCID identifier: https://orcid.org/0000-0002-2882-0874

Abstract

Analysis of the incisor enamel microstructure of extinct and extant West Indian caviomorph rodents emphasizes a clear microstructural distinction between the Echimyidae (Capromyinae and Heteropsomyinae) among Octodontoidea and the "Heptaxodontidae" whose phylogenetic affinities are debated. All capromyines and heteropsomyines have a pattern of enamel characterized by a rectangular crystallite arrangement, which is biomechanically strongest in limiting crack propagation most efficiently (subtype [Sbt.] 3 of multiserial Hunter-Schreger bands [HSBs]). This enamel condition is exclusive to all mainland octodontoids. In stark contrast, “heptaxodontids” sampled here exhibit much less derived enamel subtypes of multiserial HSBs with parallel to acute angular crystallite arrangement (Sbt. 1 [*Clidomys*], Sbt. 1–2 [*Elasmodontomys*], and low acute Sbt. 2 [*Amblyrhiza*]), less well adapted for prevention of crack propagation. The incisor enamel microstructure of *Amblyrhiza* and *Clidomys* is consistent with a chinchilloid assignment, as reflected by the anatomy of their auditory region and their unusual dental pattern. For *Elasmodontomys*, the primitive condition of its incisor enamel is difficult to reconcile with its highly nested phylogenetic position within the Octodontoidea clade (among the Capromyinae), as recently inferred from aDNA analyses. The different enamel patterns among extinct and extant West Indian caviomorphs indicate distinct high-level taxonomic groups, but restricted to the Octochinchilloi (Octodontoidea and Chinchilloidea) among Caviomorpha. The great diversity of caviomorphs on the Caribbean islands resulted from intra-archipelago diversification through time, but their high-level phylogenetic diversity can only be explained by distinct sources, implying *de facto* multiple (potentially time-staggered) natural colonizations of the West Indies. The chinchilloid-compatible enamel and dental pattern characterizing *Borikenomys* from lower Oligocene deposits in Puerto Rico, strongly suggest a link with some of the recently-extinct "heptaxodontids" that would substantiate their much greater antiquity in the Caribbean islands.

Keywords Caribbean Islands, Caviomorpha, Rodentia, Multiserial enamel, Systematics

Statements and Declarations The authors declare no competing financial interests.

Acknowledgments We are indebted to Jonathan I. Bloch (Florida Museum of Natural History, Gainesville, USA) for access to the paleontological collections of his institute, as well as S. Diaz Franco (Cuba) for the donation of his collection to one of us (LWVL). Many thanks to Thomas Martin (*Universität Bonn*, Germany) for his useful advice regarding the enamel microstructure of rodent incisors and for sharing enamel microstructure data over the last few decades. We are very grateful to our fossil preparator, Anne-Lise Charruault (ISE-M, France), for her availability and for the preparation and handling of the epoxy resin for the embedding of the incisor specimens, as well as for the access to the polishing facilities of the lab. We warmly thank Chantal Cazevieille (*Institut des Neurosciences de Montpellier* [INM], France) for access to an electron microscope scanning facility, and also for her welcome and much appreciated help in obtaining detailed images of enamel microstructures. Thank you very much to Odile Maincent (Devé, Saint-Barthélemy, French West Indies) for her hospitality and help during our successive field seasons in Saint-Barth, and for her great interest in our work. We extend our gratitude to Iván Quintero and Ángel Acosta-Colón for assistance with localities in Puerto Rico. We are also grateful to our colleagues François Pujos (IANIGLA, Mendoza, Argentina), Hernán Santos-Mercado (UPRM, Mayagüez, Puerto-Rico), Eduardo J. Cruz (UPRM, Puerto Rico), our late colleague and friend Gilles Merzeraud (*Géosciences* Montpellier, France), Mélody Philippon and Jean-Jacques Cornée (*Géosciences* Montpellier & Pointe-à-Pitre [Guadeloupe, French West Indies]), who contributed to some of the fieldwork seasons in Puerto Rico and Saint-Barthélemy in the framework of the GAARAnti project. Finally, we thank Thomas Martin (*Universität Bonn*, Germany), Daniela Kalthoff (Associate Editor; The Swedish Museum of Natural History, Sweden) and another anonymous reviewer, who provided formal reviews of this manuscript that enhanced the final version. This is ISE-M publication 2022-188 SUD.

Funding This research was supported by the French *Agence Nationale de la Recherche* (ANR) in the framework of the GAARAnti project (ANR-17-CE31-0009) and LabEx CEBA (ANR-10-LABX-25-01).

Data Availability Statement Incisor specimens analyzed (polished cross sections and remaining parts of incisors) during the current study are available from the institutions that provided them (see specimen catalog numbers). The figured and extra SEM micrographs generated and analyzed during the current study are available from the corresponding author upon reasonable request.

Introduction

Rodents are the most diverse and speciose group of living placental mammals (Wilson and Reeder 2005; Burgin et al. 2018). Much of the diversity of rodents is found among the hystricognaths of the Neotropics: the caviomorphs (Caviomorpha Wood, 1955), with emblematic forms such as the guinea pigs, capybaras, New World porcupines, chinchillas, spiny rats, or the West Indian hutias. Two main clades are recognized, each divided into two superfamilies (e.g., Fabre et al. 2015; Upham and Patterson 2015; Boivin et al. 2019a): Erethicavioi Boivin, 2019 (comprising Cavioidea Fischer, 1817 + Erethizontoidea Bonaparte, 1845 + stem-lineages) and Octochinchilloi Boivin, 2019 (comprising Chinchilloidea Bennett, 1833 + Octodontoidea Waterhouse, 1839 + stem-lineages). Caviomorphs can be found in a variety of environments, and their great taxonomical diversity is also ecological, primarily illustrated by a wide range of body-size (from about 100 g to 65 kg; e.g., Álvarez et al. 2017 and references therein), which results in a large array of lifestyles (arboreal, fossorial, semi-aquatic, and terrestrial; e.g., Mares and Ojeda 1982; Patton et al. 2015; Wilson et al. 2016), distinct locomotor behaviors (cursorial, scansorial, swimmers, etc.; Wilson and Geiger 2015; Ginot et al. 2016), different activity patterns (nocturnal, diurnal, cathemeral; e.g., Wilson et al. 2016), and different diets (e.g., Townsend and Croft 2008; Robinet et al. 2020, 2022, and references therein). This astonishing taxonomical and ecological richness of present-day caviomorphs reflects the past 35 million years (at least) of endemic evolution on the South American continent. Their fossil record so far extends back to the Eocene epoch (e.g., Antoine et al. 2012, 2016, 2021; Boivin et al. 2017, 2019a, 2022), initially limited to the tropical forested low latitudes of South America, then rapidly expanding into all higher latitude environments on the South American continent (for a review, see Boivin et al. 2019a), and even to the northeastern Caribbean islands by the early Oligocene (Vélez-Juarbe et al. 2014; Marivaux et al. 2020).

West Indian caviomorphs have long been the subject of much debate, not only to explain when and how they arrived/dispersed into these remote islands (over-water *versus* over-land dispersals), but also with regards to their phylogenetic affinities with South American groups (e.g., MacPhee and Iturralde-Vinent 1995, 2005; Woods et al. 2001; Dávalos 2004; Hedges 2006; MacPhee 2011; Marivaux et al. 2020). Extant representatives of the West Indian caviomorphs are the hutias, all members of the Echimyidae Octodontoidea, and today recognized as a single subfamily: Capromyinae (e.g., Courcelle et al. 2019). Most of the

hutias are threatened with extinction in the Greater Antilles, an IUCN's assessment that is particularly concerning given that these rodents are already the only remnants of a much greater past diversity of caviomorphs on these islands. Several species of hutias have indeed recently become extinct (e.g., MacPhee 2009; Cooke et al. 2017; Turvey et al. 2017; Upham and Borroto-Páez 2017; Orihuela et al. 2020), but so have other endemic West Indian caviomorphs, such as the heteropsomyine echimyids and the iconic "giant hutias", also known as the "Heptaxodontidae". The latter inhabited distinct Caribbean islands, and provide examples of insular gigantism, with notably a taxon that reached spectacular body size (~200 kg; Biknevicius et al. 1993), the famous *Amblyrhiza inundata* (Anguilla Bank; Cope 1868, 1883; Schreuder 1933). Other known West Indian "heptaxodontids" were not as large, but were nevertheless of respectable size (i.e., medium-sized), with *Elasmodontomys obliquus* (Puerto Rico; Anthony 1916, 1917, 1918, 1927), *Quemisia gravis* (Hispaniola; Miller 1929; Ray 1965), *Clidomys osborni* (Jamaica; Anthony 1920; MacPhee 1984; Morgan and Wilkins 2003), *Xaymaca fulvopulvis* (Jamaica; MacPhee and Flemming 2003), and possibly *Tainotherium valei* (Puerto Rico; Turvey et al. 2006). The content and high-level systematics of the "Heptaxodontidae" have been in a state of flux over the decades. They were originally regarded as a subfamily of Chinchillidae (Anthony 1917, 1918), then subsequently a subfamily closely related to the extinct large/giant South American taxa such as Eumegamyinae, Neoepiblemyinae and Phoberomyinae (these last three subfamilies were considered at that time as Cavioidea; Simpson 1945), then closely related to the Dinomyidae (Ray 1965, but see also Miller and Gidley 1918), or even a full-fledged family including only West Indian taxa, closely related to the other West Indian rodents, the Capromyidae (e.g., Woods and Hernanson 1985; Woods 1989). Some other rodentologists even kept the family in open nomenclature (*incertae sedis*) among Caviomorpha (Patterson and Wood 1982; Fabre et al. 2015), while others iteratively regarded Heptaxodontidae together with Capromyidae as Octodontoidea (McKenna and Bell 1997), also redistributing on this occasion the aforementioned related subfamilies of extinct giant rodents of South America among the standard superfamilies (for a detailed summary, see MacPhee 2011). In his study of basicranial morphology, MacPhee (2011) has found morphological evidence in favor of the chinchilloid[1] status of *Amblyrhiza*, whereas for *Elasmodontomys*, its affinities have remained uncertain inasmuch as the primitive basicranial features observed in this taxon resemble "a

[1] Chinchilloidea in its modern view, i.e., including Chinchillidae (Chinchillinae and Lagostominae), Dinomyidae and fossil kinds, and all the extinct close relatives, notably the giant neoepiblemids; e.g., Kramarz et al. 2013; Kerber et al. 2017, 2018, 2019; Rinderknecht et al. 2018; Boivin et al. 2019a; Rasia et al. 2021).

wide variety of other taxa" (but not chinchilloids in general). Yet, without much conviction, MacPhee (2011) goes with the idea that the most likely position of *Elasmodontomys* is within the Octodontoidea.

Most of the extinct capromyines, heteropsomyines and "heptaxodontids" are known from Quaternary material, although their evolutionary history on the islands undoubtedly goes back much further (MacPhee and Iturralde-Vinent 1995; MacPhee et al. 2003; MacPhee 2009, 2011). Recent gene-based phylogenies of extant Echimyidae (including West Indian capromyines and South American echimyines and euryzygomatomyines) indicate an early/middle Miocene divergence of hutias from their mainland sister taxon *Carterodon*, a result which hence suggests a Neogene colonization of the West Indies by South American octodontoids (Fabre et al. 2014; Courcelle et al. 2019). Even more recent molecular phylogenetic analyses of Neotropical Echimyidae, including extant capromyines and, for the first time, ancient DNA (aDNA) of extinct capromyines and heteropsomyines plus *Elasmodontomys*, resolved the latter taxon as closely related to the Hispaniolan capromyine *Plagiodontia*, both taxa being situated at the base of the Capromyinae clade (Woods et al. 2020). Extinct heteropsomyines sampled for these analyses (*Boromys offella* and *Brotomys voratus*) were found as the closest out-groups of the Capromyinae clade (Woods et al. 2020). In this phylogenetic context, the identification of such a West Indian clade gathering heteropsomyines + capromyines-*Elasmodontomys*, led Woods and colleagues to consider the origin of these rodents as the result of a single event of colonization of the Caribbean archipelago from a South American *Carterodon*-like echimyid ancestor, sometime during the early/middle Miocene interval. Although the title of their publication[2] entails the monophyly of all West Indian caviomorphs, they also suggested that other "heptaxodontids", notably *Amblyrhiza* and/or *Clidomys*, might represent (a) separate colonization(s) of the West Indies by other mainland caviomorphs, albeit no Miocene or Quaternary South American caviomorph is known to be closely related to these two West Indian subfossils to date.

The direct evidence of an ancient dispersal of South American caviomorph rodents toward the Caribbean archipelago was first provided by the discovery of dental remains of an echimyid octodontoid from the early Miocene of Cuba (*Zazamys veronicae*; MacPhee and Iturralde-Vinent, 1995). The subsequent discovery of a rodent incisor in lower Oligocene deposits in Puerto Rico (Río Guatemala [RG], San Sebastian Formation [SB Fm.])

[2] "*Ancient DNA suggests single colonization and within-archipelago diversification of Caribbean caviomorph rodents*" (Woods et al. 2020).

demonstrated that rodents had colonized the Greater Antilles even earlier (Vélez-Juarbe et al. 2014). Interestingly, the enamel microstructure of that incisor indicated the presence on this island, at that early time, of a caviomorph with affinities other than Octodontoidea (i.e., rather chinchilloid, cavioid or erethizontoid affinities; Martin in Vélez-Juarbe et al. 2014). In 2019, the additional discovery of several dental remains (molars) in these same Puerto Rican deposits (RG, SB Fm.), compatible in size to the former incisor found in the same spot, have allowed to demonstrate the presence of undoubted chinchilloid rodents in Puerto Rico as early as the early Oligocene (Marivaux et al. 2020). This discovery has therefore raised the critical question of a possible link between these Paleogene Puerto Rican chinchilloids and some of the Pleistocene–Holocene West Indian "giant hutias" ("heptaxodontids", especially *Amblyrhiza* and *Elasmodontomys*) for which a chinchilloid status was also supported from compatible dental morphology and incisor enamel microstructure evidence (Marivaux et al. 2020). Accordingly, the possibility of a greater antiquity of some of the Quaternary "giant hutias" has been seriously considered, as well as the existence of a pattern of multiple and time-staggered dispersal events to explain the natural colonization of the West Indies by rodents (see Marivaux et al. 2020, 2021).

We explore here the possible link between the Oligocene Puerto Rican chinchilloids and some of the Pleistocene–Holocene West Indian "heptaxodontids" (after Marivaux et al. 2020) *versus* the relationships between "heptaxodontids" and capromyine/heteropsomyine octodontoids (after Woods et al. 2020), through the analysis of the incisor enamel microstructure. This study substantially complements taxonomically Martin's (1992) first analysis of incisor enamel microstructure of West Indian caviomorph subfossils, and provides illustrations of the enamel of these taxa, which had not been made available previously (notably for *Amblyrhiza* and *Elasmodontomys*, and the few hutias sampled initially). The enamel microstructure of the incisor of rodents has proven to be a powerful tool for systematics and phylogeny of the group (e.g., Korvenkontio 1934; Wahlert 1968; Boyde 1978; Koenigswald 1985; Martin 1992, 1993, 1994a, b, 1997; Kalthoff 2000; Marivaux et al. 2004).

The incisor enamel in rodents is primarily composed of two layers (Korvenkontio 1934), the *portio externa* (PE) consisting of radial enamel in which bundles of hydroxyapatite crystallites (= prisms) are oriented in the same direction, and the *portio interna* (PI), which is characterized by decussating bands of prism rows, named Hunter-Schreger bands (HSBs) (Martin 1992, 1993; Koenigswald and Sander 1997; Alloing-Séguier et al. 2019). Between the

prisms, there is an enamel fraction also formed by parallelly-oriented hydroxyapatite crystallites, but which are not bundled into prisms (Fig. 1). This fraction forms the inter-prismatic matrix (IPM). Ctenohystrican rodents (including Ctenodactylidae, Diatomyidae, and Hystricognathi) display an incisor enamel layer with a PI having decussating multi-prism rows and thin sheets of IPM, which allows describing multiserial HSBs (Korvenkontio 1934; Martin 1992, 1993). On the basis of the angle of the IPM crystallites with respect to the prism long axes, several subtypes of multiserial HSBs can be distinguished (Martin 1992, 1993, 1994a, 1997; see Boivin et al. 2019b). A first subtype (Sbt. 1) can be described when the IPM crystallites run parallel to those of the prisms, or slightly deviate from them with a low angle (very low acute angle), and anastomoses very regularly, but without totally surrounding each prism (sheet to sheath-like IPM). A second subtype (Sbt. 2) is identified when the IPM crystallites (thin sheets) anastomose moderately to regularly, and form an acute angle (with a wide amplitude range) to the prism crystallite direction. A third subtype (Stb. 3) is described when the IPM sheets show few or no anastomoses, and their crystallites run at a very high acute or right angle to those of the prisms, forming inter-row sheets (i.e., rectangular plate-like IPM; Fig. 1). On the biomechanical level, an increasing angulation of the IPM provides a better resistance to the crack propagations, as it strengthens the enamel in the third dimensions (Martin 1992, 1993, 1994a, 1997). A Sbt. 3 of multiserial HSBs characterized by such a rectangular crystallite (prisms and IPM) arrangement is considered as the most derived/specialized condition of enamel, a statement which is corroborated by the successive stratigraphic occurrences of the different subtypes (1 then 2 and finally 3), and the observation of transitional cases (i.e., Sbt. 1–2 and Sbt. 2–3; Martin 1994a, 1997, 2005; Marivaux et al. 2004, 2019; Vucetich et al. 2015; Boivin et al. 2019b). The three subtypes of multiserial HSBs can be found in the different main ctenohystrican clades (see Online Resource 1), with the Sbt. 3 iteratively acquired in most terminal clades. Among caviomorphs, the Sbt. 1, Sbt. 2 and transitional Sbt. 1–2 of multiserial HSBs are found in extinct and extant erethizontoids, chinchilloids and cavioids (Online Resource 1; Martin 1992, 1994b). Modern members of these last three superfamilies have then preserved less advanced and less resistant incisor enamel conditions. In contrast, the derived transitional Sbt. 2–3 and chiefly Sbt. 3 of multiserial HSBs are restricted to octodontoids from an early stage in their evolutionary history (Online Resource 1; Martin 1992, 1994b, 2004, 2005; Boivin et al. 2019b). However, the achievement of Sbt. 3, which can be seen as the best adaptation against crack, seems to have evolved rapidly and iteratively within the Octodontoidea clade (e.g., Vucetich and Vieytes 2006; Vucetich et al. 2010; Boivin et al. 2019b). This incisor enamel condition (Sbt.

3) characterizing virtually all extinct and all extant octodontoids is therefore particularly in stark contrast to the less advanced enamel condition observed by Martin (1992) for the incisor of *Elasmodontomys* (i.e., low acute Sbt. 2; Martin 1992 [but not illustrated]), especially if the latter taxon turns out to be nested high within the Octodontoidea clade, well-into the Echimyidae, as resolved by Woods et al. (2020).

For the purposes of this study, we assembled an important number of incisors of extinct West Indian caviomorphs, including a newly-discovered incisor of the chinchilloid from the early Oligocene of Puerto Rico, and several incisors documenting "heptaxodontids", heteropsomyines and capromyines, which all come from Quaternary contexts (see Table 1). With this sampling, we have the opportunity to compare more comprehensively than Martin (1992) the incisor enamel microstructure characterizing each West Indian caviomorph group, to highlight some incompatibilities of previously suggested phylogenetic affinities, and finally to discuss in favor or against some recently proposed phylogenetic hypotheses concerning "giant hutias". We will discuss the results with a special emphasis on the implications for macroevolutionary and historical biogeographic patterns of some West Indian caviomorphs.

Materials and Methods

The material of this study consists primarily of incisors of subfossil and fossil caviomorphs from the West Indies, which have been recovered over the past few decades (see Table 1 for details on their geographic provenance, age and collectors/collections). We assembled incisors documenting subfossil "heptaxodontids" (notably *Amblyrhiza*, *Elasmodontomys*, and *Clidomys*), subfossil heteropsomyines (*Heteropsomys*, *Boromys*, and *Brotomys*), and subfossil capromyines (*Isolobodon*, *Hexolobodon*, *Rhizoplagiodontia*, *Plagiodontia*, *Geocapromys*, *Capromys*, *Macrocapromys*, and *Mesocapromys*), the two latter being echimyid octodontoids. We tried to sample as many genera as possible, represented by at least one species (at best two). Regrettably, we were not successful in obtaining incisors documenting the extinct "heptaxodontid" *Quemisia*, *Xaymaca*, and *Tainotherium*. An incisor recovered from lower Oligocene deposits of Puerto Rico (San Sebastian Fm.) was also sampled for enamel microstructure analyses. This incisor was found in the same level as the former one described by Vélez-Juarbe et al. (2014) and the lower molars of compatible size that allowed the description of a dinomyid chinchilloid (*Borikenomys*; see Marivaux et al. 2020). Incisors of a

few living caviomorphs from South America (*Chinchilla* and *Lagidium* [chinchillid chinchilloids], and *Cuniculus* [cuniculid cavioid]) and from the West Indies (*Mysateles* [capromyine]) were also sampled here for enamel comparison purposes. The latter were retrieved from skulls of available specimens housed in the osteological collection of the *Université de Montpellier* (Table 1). However, our primary reference for enamel microstructure comparisons will be the extensive database of incisor enamel of living caviomorphs assembled by Martin (1992). The latter also includes enamel data on extinct caviomorphs, as well as other extant and extinct rodents in general (Online Resource 1). This database for comparisons will be supplemented by the subsequent work of Martin (1993, 1994a, 1994b, 2004, 2005), and other available work on this topic (e.g., Vieytes et al. 2007; Vucetich et al. 2010, 2015; Arnal et al. 2014; Vélez-Juarbe et al. 2014; Assemat et al. 2019; Boivin et al. 2019b; Marivaux et al. 2019, 2020). For our sampling, in most cases (extinct and extant species), the incisors were removed from the embedding bone structure (dentary or maxillary), and only a fragment of less than 1 cm was punctured for analysis. The remaining part of the incisor was repositioned in the bone socket, or preserved separately. In some fossil cases, incisors or fragments of incisors were found isolated. In fossil rodent-bearing localities containing several species, incisor identification was made by morphological comparison with better-preserved specimens from the same localities, whose bony structures bear incisors and molars, as well as on the basis of size compatibility. Lower *versus* upper incisors were identified according to their radius of curvature (lower incisors having a much greater radius than upper incisors of similar overall dimensions).

All selected incisor specimens were embedded in artificial epoxy resin. After hardening, they were cut transversally to observe the incisor in cross-section, and to draw the outline of the enamel layer (Fig. 2). They were subsequently grounded and polished longitudinally with successive silicon carbide papers (800–4000). The final finely polished sections were etched for 30 s with 37% phosphoric acid (H_3PO_4), to make the microstructural details of the enamel visible, then rinsed with distilled water. The samples were air-dried and coated with conductive material (palladium) before being examined with a scanning electron microscope (SEM; HITACHI S 4000) at different magnifications (Figs. 1 and 3–9).

For describing the enamel microstructure, we followed the nomenclature of Koenigswald and Sander (1997) and Martin (1992, 1993) (see Fig. 1). The measurements carried out on the enamel layer observed in longitudinal section follow those proposed by Martin (1992, 1993), Boivin et al. (2019b) and Marivaux et al. (2019). The angle α formed between the direction of

the IPM crystallites and that of the prism crystallites was measured at the level of the HSB, where the prism axis is the longest. For describing the variation of α across the different incisor sampled, we arbitrarily subdivided its observed range as follows: $0° \leq \alpha \leq 15°$, the IPM crystallites and the prism crystallites are parallel or their respective directions deviate slightly from each other, forming a very low acute angle; $15° < \alpha \leq 40°$, the directions of the two crystallite sets form a low acute angle; $40° < \alpha \leq 70°$, they form a medium to high acute angle; $70° < \alpha \leq 90°$, they form a very high acute to right angle (rectangular crystallite arrangement, plate-like IPM). The identification of a subtype of multiserial HSBs for a given incisor was based on the observation of the whole longitudinal section available of the specimen. The distinction between the main subtypes (and subtle cases of transitional subtypes) was based not only on the value of α, but also on the general organization/configuration of the IPM (i.e., sheets between rows of prisms, sheets inter-prisms, sheath-like sheets, and frequency of the IPM crystallite anastomoses). We note that the recognition of transitional subtypes (especially Sbt. 1–2) is subtle and sometimes difficult to formalize. Nevertheless, we primarily considered the apparent increase in resistance to crack propagation (otherwise, the primitive state as opposed to the successive more advanced/derived states of the IPM configuration, more efficient to limit crack propagation).

Results

All the incisors analyzed (25) in longitudinal section exhibit a double layer enamel consisting of a PE of variable thickness from one tooth specimen to another and composed of radial enamel, and a PI showing decussated multi-prism rows and thin IPM sheets, which allows the description of multiserial HSBs (Figs. 3–9). All observed enamel characters and measurements made on SEM photographs of the studied incisor specimens are reported in Table 2.

Capromyinae Echimyidae Octodontoidea

Isolobodon portoricensis † (Fig. 3a–b) **and *I. montanus*** † (Fig. 3c–d). For both species, the enamel layer in longitudinal section displays HSBs in PI that run straight. The PE, with radial

enamel, is weakly extensive, representing only about 1/10th or less of the enamel thickness. In *I. montanus*, the prisms in PE are strongly inclined and lanceolate. In both species, HSBs in PI display four prisms in average per band, which are oval to flattened in cross-section. A prism of transition between two decussating HSBs can be observed on *I. portoricensis*, whereas it is not clearly visible/identifiable on *I. montanus*. The IPM crystallites in PI are less developed than those of the prisms, whereas in PE it seems equal in strength. In PI, the IPM is thin and lies plate-like between the prism rows (i.e., inter-row sheets), without anastomosis, and with its crystallite direction nearly perpendicular to the prism main axes. With such an IPM crystallite arrangement, the two incisors of these two species of *Isolobodon* illustrate an enamel microstructure characterized by an advanced Sbt. 3 of multiserial HSBs. The enamel layer differs only moderately between the two species, notably in overall thickness (PE + PI), which is thinner in *I. montanus* (although the incisor is slightly wider), and in the presence of more inclined HSBs in PI in *I. portoricensis*.

Hexolobodon phenax † (Fig. 3e–f). The enamel layer is particularly thick with respect to the width of the incisor (compared to the thickness observed in other capromyines with incisors of comparable size). The PE is limited, accounting for less than 10% of the total enamel thickness. The PI/PE boundary is straight and clearly perceptible. In PI, the HSBs are inclined at ~25° (main axis), but they are not straightly arranged from the EDJ to the PI/PE boundary, and instead appear somewhat undulating. Near the EDJ (~15% of PI) and the PI/PE boundary (~5% of PI), the HSBs are more inclined than in the main central part of PI. Each HSB display four prisms that are particularly flattened in cross-section, and there is no prism of transitional zone between two adjacent HSBs. The IPM crystallites run at a nearly right angle to the prism crystallites, and form thin sheets (plate-like) between rows of prisms (inter-row sheets), with only very rare anastomoses. This kind of crystallite arrangement typifies a Sbt. 3 of multiserial HSBs.

Rhizoplagiodontia lemkei † (Fig. 3g–h). The enamel layer of this taxon is almost entirely composed of PI, the PE being less than 5%. Furthermore, the PE/PI boundary remains particularly difficult to distinguish. In PI, the HSBs are markedly inclined and straightly arranged, and are composed of three or four oval to flattened prisms, the fourth being often a prism of transitional zone between two HSBs. At the EDJ, a thin starting zone with a parallel prism progression is observable. The IPM crystallites in PI are almost perpendicular to the

crystallites of the prisms, and form thin plates between the prism rows (i.e., inter-row sheets), without any perceptible anastomosis. This type of crystallite arrangement typifies a Sbt. 3 of multiserial HSBs.

Plagiodontia ipnaeum † (Fig. 4a–b). Whereas this taxon is the largest of the West Indian echimyids sampled (capromyines and heteropsomyines), its (large) incisor displays a particularly thin enamel layer, almost similar in thickness to that of taxa with incisors almost twice as small (see Table 2, Incisor width *versus* Enamel thickness). The PE is limited (~8% of the total enamel thickness), and the PI/PE boundary is straight and clearly perceptible. In PI, HSBs are moderately inclined, and are composed of at least four prisms that are oval in cross-section. There is an additional prism that appears as a transitional zone between two HSBs. The crystallites of the IPM and prisms are of equal strength. The direction of the IPM crystallites forms a right angle with the main axis of the prisms. The IPM lies plate-like, forming well-marked and separated sheets between prism rows (no anastomosis), thereby describing a typical Sbt. 3 of multiserial HSBs.

Capromys pilorides lewisi † (Fig. 4c–d). This taxon displays a tick enamel layer relative to the incisor proportions. The PE is limited and the PE/PI boundary is not well defined. In PI, the HSBs are slightly inclined, appearing nearly sub-vertical near the EDJ (accounting for 5% of PI). At least five or even six prisms, arranged in a row, can be counted across the width of a HSB. There is no visible transitional prism between two HSBs. The IPM crystallites run perpendicular to those of the prisms, forming thin inter-row sheets, which never anastomose. This type of crystallite arrangement typifies a well-accomplished Sbt. 3 of multiserial HSBs.

Geocapromys caymanensis † (Fig. 4e–f) **and** ***G. columbianus*** † (Fig. 4g–h). The two incisors sampled in these two species of *Geocapromys* have the same size, and also display a similar thickness of their enamel layer, which may seem relatively thin compared to other capromyines of similar incisor size (Table 2). In both species, the PE is strongly reduced and hardly discernible. In PI, the HSBs are strongly inclined, and include rows of four to five prisms in width, without prism of transitional zone. The prisms are oval in cross-section. The crystallite (IPM and prisms) arrangement in PI is basically similar in the two species. The IPM is well marked and appears as well-defined sheets between the prism rows (plate-like),

without IPM inter-prism crystallite in a row (i.e., without anastomosis or very rarely). The crystallites of the IPM sheets run at an almost right angle to the main direction of the prisms. Both species of *Geocapromys* exhibit an incisor enamel microstructure characterized by a Sbt. 3 of multiserial HSBs.

Macrocapromys acedo † (Fig. 5a–b). The analyzed incisor has a thin enamel layer, with a relatively narrow but clearly distinguishable PE of radial enamel, characterized by strongly bent prisms. In PI, the HSBs are only slightly inclined (barely 23°) and straight, with only three prisms wide (in row), and a fourth being a prism of transitional zone between two HSBs. The prisms are strongly flattened, and can even be confused with the IPM sheets (inter-row plate-like), inasmuch as the IPM and prism crystallites seem equal in strength. The IPM crystallites run fully perpendicular to the main direction of the prism crystallites, without any anastomosis. This crystallite arrangement describes a Sbt. 3 of multiserial HSBs.

Mesocapromys nanus † (Fig. 5c–d). The sampled incisor has a "standard" thickness of its enamel layer (i.e., neither thicker nor thinner than the average of all sampled capromyine incisors). It displays a well-developed PE that accounts for about 15% of the total enamel thickness, a feature that distinguishes this genus (as well as *Mysateles*) from other sampled capromyines showing a thinner PE development. The radial enamel of the PE includes prisms and IPM parallel and steeply inclined (almost horizontal). In PI, HSBs are particularly inclined (~50°). The prisms (limited to three per band) are very flattened, and their crystallites seem of equal strength to those of the IPM sheets. There is a well-defined prism of transitional zone between two adjacent HSBs. The IPM crystallites run at a very high acute angle (sub-rectangular) to the prism direction. There is no IPM inter-prism crystallite anastomosis between prism rows. The enamel microstructure of this incisor documents a Sbt. 3 of multiserial HSBs.

Mysateles **sp.** (Fig. 5e–f). The incisor enamel of this genus is very close to that of *Mesocapromys*, with a proportionally similar thickness of the enamel layer (with respect to the incisor width), including a well-developed PE (16%). Crystallites of prisms and IPM in PE are parallel and steeply inclined. In PI, HSBs are inclined at 35°. They include well-defined and parallel rows composed of three to four prisms, which are particularly flattened.

The fourth prism of the row can be a prism of transition between two adjacent HSBs, but the latter is neither well-marked nor regular. The crystallites of the prisms are of equal strength to those of the IPM sheets. The latter are well distinguished, and their crystallites run fully perpendicular to the prism direction, with no inter-prism or inter-row anastomosis. Such a crystallite arrangement describes a well-accomplished Sbt. 3 of multiserial HSBs.

Heteropsomyinae Echimyidae Octodontoidea

Brotomys contractus † (Fig. 6a–b). This small upper incisor displays a moderately thin enamel layer, with a well-marked PE of radial enamel accounting for 12 % of the total enamel thickness. The prisms in PE are parallel and strongly inclined, nearly oriented horizontally. The PI/PE boundary is straight but not well defined linearly, with HSBs in PI protruding irregularly in the PE zone. In PI, HSBs are only slightly inclined (~20°), straight and include successive rows including a maximum of three prisms, which are rounded to oval in cross-section. One to two prisms form a well-marked transitional zone between two adjacent HSBs. The IPM form thin inter-row sheets (plate-like IPM), whose crystallites have a perpendicular orientation to those of the prisms. There is no anastomosis of the IPM sheets. This crystallite arrangement describes a Sbt. 3 of multiserial HSBs.

Boromys offella † (Fig. 6c–d) **and** ***B. torrei*** † (Fig. 6e–f). These two small incisors document two species of *Boromys*, particularly tiny, among the smallest of the species sampled for these analyses. As is the case with *Brotomys*, considering the size of these two incisors (in relation to the measured incisor width), their enamel layer may appear relatively thick compared to the condition observed in capromyines. Both incisors have a PE representing 10–12% of the total enamel thickness. The PE/PI boundary is particularly difficult to distinguish, especially for the incisor of *B. offella*, inasmuch as the prisms and IPM are of similar strength, parallel and vertically oriented. This portion of the incisor enamel of *B. torrei* was damaged by polishing, which does not allow for a clear observation of the crystallite orientation in PE. In PI, for both incisors, the HSBs display regular rows including three to four prisms appearing relatively flat in cross-section, the fourth prism forming a well-marked transitional zone between two adjacent HSBs. In both specimens, the IPM lies plate-like between the prism rows (i.e., inter-row sheets), without clear anastomosis (eventually possible but rare for *B. offella*). The IPM

crystallite direction is perpendicular to the prism main axis. The enamel microstructure of these two incisors is basically similar and describes a well-accomplished Sbt. 3 of multiserial HSBs. The enamel of the two incisors differs in the inclination of the HSBs in PI, which appear more inclined in *B*. *offella* than in *B*. *torrei*, although these differences in inclination might simply reflect a difference in the sampled dental locus (lower *versus* upper incisor, respectively). They also differ in the presence of rare HSB divisions, noticeable in *B*. *torrei*, but not observed in *B*. *offella*.

***Heteropsomys* sp. †** (Fig. 6g–h). Considering the size of this sampled incisor, which is more than twice as large as the incisors of *Brotomys* and *Boromys*, the incisor enamel layer in *Heteropsomys* is particularly thin, similar to that of the incisor of *B*. *torrei*, the smallest species sampled here (see Table 2). PE accounts for 10% of the total enamel thickness, and includes prisms and IPM of similar strength, parallel and strongly inclined. The PE/PI boundary is clearly distinguishable and straight. In PI, the HSBs are moderately inclined, straight and are composed of prism rows including four to five prisms, oval in cross-section, with the fifth prism forming a transitional zone between two HSBs. The IPM is particularly well marked, lying plate-like between the prism rows, with possible (very rare) anastomoses. The crystallites of the IPM sheets run at a very acute to right angle (i.e., sub-rectangular) to the main direction of the prisms. This crystallite arrangement typifies a Sbt. 3 of multiserial HSBs.

"Heptaxodontidae"

***Elasmodontomys obliquus* †** (Fig. 7a–f). The three available incisors sampled for this taxon are lower ones. They are among the largest incisors in our study, reflecting the medium to large body size of *Elasmodontomys*, approximating that of the capromyine *Plagiodontia*. Despite the large size of these incisors, their enamel layer is proportionally very thin, with a thickness equivalent to that observed on incisors two to three times smaller previously studied (capromyines or heteropsomyines; Table 2). The PE of radial enamel is variable in thickness, accounting for 10 to 17% of the total enamel thickness. Prisms and IPM in PE are of similar strength, and moderately inclined. The boundary between PE and PI is quite distinct, but not smooth and horizontal, appearing somewhat rough due to the presence of HSBs of PI

protruding irregularly in the PE zone. In PI, HSBs are moderately inclined (27–37°) and straightly arranged from the EDJ to the PI/PE boundary. At the EDJ, a thin starting zone with a parallel prism progression is observable. HSBs are noticeably wide, comprising oblique rows of four to five prisms, the fifth prism or even an additional sixth prism, forms a particularly well-defined transitional zone between two adjacent HSBs. Prisms are rounded/oval to slightly flattened in cross-section. The IPM is thin but particularly "invasive", forming sheets between the prism rows and often between the prisms in a row, thereby describing a pattern of IPM characterized by regular anastomoses. The IPM crystallites run with a low but clearly discernible angular difference to the prism crystallites (low acute angle between the directions of the two crystallite sets). Such an IPM crystallite arrangement with a low value of α, describes among the early stages of a Sbt. 2 of multiserial HSBs, even a transitional Sbt. 1–2 if we consider the very frequent and regular anastomoses of the IPM sheets (inter-rows and frequently inter-prisms in a row).

***Clidomys* sp.** † (Fig. 7g–h). The incisor of this taxon is also among the largest specimens sampled, and like in *Elasmodontomys*, the enamel layer is thin, equivalent in thickness to the incisors two to three times smaller studied previously (capromyines or heteropsomyines; Table 2). The PE represents only 10% of the total enamel thickness. The IPM and prism crystallites in PE are equal in strength as no distinction can be made between the two structures. The PE/PI boundary is discernible, but somewhat discontinuous in appearance due to the presence of protruding HSBs of PI in the PE area. In PI, the HSBs are very slightly inclined (12–15°) and can split or fuse locally, but most often in a limited PI region (about 30%) situated near the PI/PE boundary. The HSBs are straight and particularly wide, composed of poorly defined rows of prisms, which may include up to five prisms (or occasionally more in the split regions or less in the merging regions). There is no clear prism of transition between two HSBs. The prisms are strongly flattened in cross-section. The IPM crystallites form thin sheets that run partly parallel to the prisms, but also partly at a very low angle. The IPM sheets anastomose permanently, so that the prisms are almost completely enveloped (sheath-like IPM). Due to a very close direction of the IPM and prism crystallites, it may be difficult to distinguish the two structures in cross-section. Such a crystallite arrangement with almost parallel prisms and IPM sheets, the latter anastomosing permanently, corresponds to a Sbt. 1 of multiserial HSBs.

***Amblyrhiza* sp. †** (Fig. 8a–d). The incisor of this taxon is the largest specimen sampled for this analysis, reaching at least twice the size of the incisor of *Clidomys*, and more than twice the size of some of the incisors of *Elasmodontomys*. The thickness of the enamel layer is of the same importance as the incisors of *Clidomys* and *Elasmodontomys*, thereby indicating a relatively thin enamel layer for the size of the incisor, compared to the sampled echimyids (capromyines and heteropsomyines). The PE with radial enamel accounts for 10–13% of the total enamel thickness, including prisms and IPM of similar strength, and as such being not clearly distinguishable from each other. The PE/PI boundary is fairly distinct, but not clearly delineated. In PI, the HSBs are straight and moderately inclined (25–34°), and no division was observed along the analyzed section. The HSBs are rather large, showing inclined multi-prism rows, comprising at least five prisms per band, plus one or two prisms of transition between two adjacent HSBs (not on a regular basis). The prisms have an oval or flat cross-section. The IPM is relatively thick with respect to the prism, and thus well visible, forming sheets between the prism rows and often between the prisms in a row, indicating frequent and regular anastomoses. The crystallites of IPM run at a low acute angle to the prism direction. This crystallite arrangement describes an early stage of a Sbt. 2 of multiserial HSBs.

***Amblyrhiza* sp. † (juvenile)** (Fig. 8e–f). This medium-sized incisor was found in the same fossil locality (and in close proximity) as the one that yielded the large-sized remains attributed to *Amblyrhiza* (Îlet Coco, St. Barth; Table 1). It is almost half the size of the largest *Amblyrhiza* incisors recovered, and its buccal surface is characterized by a crenulated ornamentation, similar to that of the large incisors of the genus. Given that there is no other large-bodied caviomorph rodent other than *Amblyrhiza* recorded/known on the Anguilla Bank to date, it is likely that this smaller incisor specimen corresponds to a juvenile individual of *Amblyrhiza* (*inundata*?). The microstructural pattern in PI (crystallite arrangement of the prisms and IPM) is indeed strictly similar to the one described above (i.e., early stage of Sbt. 2 of multiserial HSBs). The main distinctions are, of course, a thinner enamel layer, but especially the shape and inclination of the HSBs. The latter appear as curved (with a high radius of curvature). They are strongly inclined in the central part of PI, while they become almost vertical when approaching the EDJ.

Fossil Chinchilloidea and living Chinchilloidea and Cavioidea

Borikenomys praecursor † (Fig. 8g–h). This incisor fragment displays a moderately thin enamel layer, but somewhat thicker than that covering the former incisor described by Martin in Vélez-Juarbe et al. (2014). Similar to the latter one, the enamel is double-layered, with a PE accounting for 18% of the total enamel thickness (among the thickest PE recorded here). In PI, HSBs are also ~40° inclined apically, and comprise three to four prisms per band, which are rounded to oval in cross-section. The fourth prism is often transitory between two adjacent HSBs. The IPM crystallites run at a low acute angle to the prism long axes, and are arranged as thin sheets (hardly visible) between the prism rows, and anastomose regularly, thereby describing an early stage of a Sbt. 2 of multiserial HSBs.

Lagidium **sp.** (Fig. 9a–b). The enamel layer of this small-bodied species is very thin (much thinner than in the smallest West Indian echimyids sampled here; i.e., *Boromys*, *Brotomys*, *Mesocapromys*, *Geocapromys*, etc.), double-layered with a rather extensive PE, accounting for 19% of the total enamel thickness (one of the thickest PE recorded here). The crystallites of the IPM and prisms are of similar strength in PE (i.e., hardly differentiable), both making structures strongly inclined. The PE/PI boundary is well distinct but not linear. In PI, HSBs are steeply inclined (45°; one of the highest angles recorded here) and straight, with three to four prisms wide, the fourth even a fifth prism being transitional between two HSBs. In cross-section, the prisms are oval to flattened. The IPM is predominantly parallel to the prism direction, but occasionally minor angular differences occur (very low acute angles). It consists of thin inter-row and inter-prism sheets (permanent anastomoses) that almost completely envelop the prisms on all sides (sheath-like IPM). Such a crystallite arrangement typifies a Sbt. 1 of multiserial HSBs, and even transitional Sbt. 1–2 if we take into consideration the minor angular differences between the direction of the IPM crystallites and that of the prism crystallites.

Chinchilla **sp.** (Fig. 9c–d). The enamel layer is, as for the incisor of *Lagidium*, very thin, with a thick PE (21%). In PE, the crystallites of the IPM and prisms are hardly differentiable, both appearing strongly inclined. The PE/PI boundary is straight/horizontal, and particularly well distinguishable. In PI, the HSBs are strongly inclined (up to 49°), straight, and include three flat prisms per band, with a well-marked transitional zone between two adjacent HSBs, made

by one or two additional prisms. The IPM form thin sheets between the prism rows and often between the prisms in a row (frequent/regular anastomoses). The IPM crystallites form a very low to low acute angle to the prism direction. This crystallite arrangement describes an earlier stage of a Sbt. 2 of multiserial HSBs (even a transitional Sbt. 1–2 if we consider the very frequent and regular anastomoses of the IPM sheets).

Cuniculus paca (Fig. 9e–f). This sampled incisor of that medium-sized caviomorph (Cavioidea) displays a moderately thick enamel layer with a PE accounting for a large part of the total enamel thickness (22%). The PE/PI boundary is clearly distinct and straight. In PI, the HSBs are only slightly inclined and include frequent divisions. The HSBs appear wide, although including only four prisms, which are large but very flattened in cross-section. There is no prism of transition between the HSBs. The IPM crystallites and prism crystallites are of similar strength, and run parallel to each other. However, it sometimes happens that their respective directions deviate slightly from each other, forming a very small acute angle. The IPM sheets anastomose on a regular basis (inter-row and inter-prism; i.e., sheath-like IPM). This crystallite arrangement corresponds to an advanced Sbt. 1 of multiserial HSBs.

Discussion and Conclusion

In this study, we substantially expanded taxonomically Martin's (1992) first analysis of incisor enamel microstructure of extinct and extant West Indian caviomorphs. Pragmatically, we especially provide here enamel SEM pictures of some of the formerly sampled taxa that had not previously been illustrated (Martin 1992; Martin in Vélez-Juarbe et al. 2014). For the taxa treated by both Martin (1992) and ourselves (plus the additional taxa in our dataset), the results are fully consistent, showing a clear distinction between the enamel microstructures of the West Indian Echimyidae Octodontoidea (Capromyinae and Heteropsomyinae) and the West Indian "Heptaxodontidae", whose phylogenetic affinities are still debated. All extinct and extant hutias and spiny rats from the West Indies (capromyines and heteropsomyines, respectively) have enamel crystallites whose configurations, assemblages and/or proportions vary in many respects (e.g., number of prisms per HSB, presence or absence of transitional prisms between HSBs, shape of the prisms in cross section, inclination of HSBs in PI, percentage of PE, etc.; see Table 2), but all describing a pattern of enamel microstructure

characterized by a rectangular crystallite (IPM and prisms) arrangement that is biomechanically strongest in limiting crack propagation (i.e., Sbt. 3 of multiserial HSBs; Table 2). This highly derived/specialized condition of the incisor enamel is found in all their echimyid octodontoid counterparts from the South American continent (i.e., Echimyinae, Euryzygomatomyinae, and Carterodontinae; Martin 1992), and more extensively in all related families within the Octodontoidea clade (i.e., Echimyidae, Octodontidae, Ctenomyidae, and Abrocomidae; Martin 1992) (see Online Resource 1). In caviomorphs in general, the Sbt. 3 of multiserial HSBs is not observed in chinchilloids, cavioids and erethizontoids (see Online Resource 1), being exclusive of octodontoids, and this from an early stage in their evolutionary history (Martin 1992, 2004, 2005; Vucetich and Vieytes 2006; Vucetich et al. 2010; Boivin et al. 2019b). Such a highly resistant/efficient enamel microstructure characterizing West Indian echimyids contrasts sharply with that recorded for the "heptaxodontid" taxa sampled here for this analysis, which exhibit much less resistant incisor enamels. Indeed, the incisors of *Clidomys*, *Elasmodontomys* and *Amblyrhiza* display an enamel layer relatively much thinner and characterized by a less complex crystallite arrangement, with the IPM sheets being parallel or at a low acute angle to the prism long axes, and permanently or regularly anastomosing. Such crystallite arrangements describe less advanced subtypes of multiserial HSBs (Sbt. 1 [*Clidomys*], Sbt. 1–2 [*Elasmodontomys*], and low acute Sbt. 2 [*Amblyrhiza*]; see Table 2). The same is true for the incisor of the chinchilloid *Borikenomys* from the early Oligocene of Puerto Rico, which displays an enamel microstructure typifying a low acute Sbt. 2 of multiserial HSBs, strongly reminiscent to that of the incisor of *Amblyrhiza* (regardless of the very large size difference between the two taxa). These less advanced enamel microstructures characterizing West Indian "heptaxodontids" (or "giant hutias") are found in extinct and extant chinchilloids, cavioids or erethizontoids from South America, but never in octodontoids (see Online Resource 1 and Table 2; Fig. 9; Martin 1992).

The absence of highly-derived rectangular crystallite arrangements in the incisor enamel of *Amblyrhiza* and *Clidomys*, does not favor of an octodontoid status for these two taxa, but, in turn, it is consistent with a chinchilloid assignment, as independently reflected by the anatomy of their auditory region (middle-ear of *Amblyrhiza*, MacPhee 2011; inner-ear of *Amblyrhiza* and *Clidomys*, Da Cunha 2020, unpublished MSc results; Da Cunha et al. in prep.) and their unusual dental pattern (e.g., Marivaux et al. 2020, and cited references herein). For *Elasmodontomys*, it is more complicated since a primitive condition of the IPM

crystallite arrangement characterizing its incisor enamel microstructure (i.e., Sbt. 1–2 of multiserial HSBs), is difficult to reconcile with the highly-nested phylogenetic position of this taxon within the Octodontoidea clade (among the Echimyidae Capromyinae), as recently inferred from aDNA analyses (Woods et al. 2020). *Elasmodontomys* was indeed found sister to *Plagiodontia* (*P. aedium*), and the subclade of both species was resolved at the base of the Capromyinae clade. Species of *Plagiodontia* (*P. aedium* and *P. ipnaeum*) are smaller-bodied than *Elasmodontomys obliquus*, but their incisors are comparatively very large and robust (Table 2). The incisor of *P. ipnaeum* (Fig. 2e) sampled here is of roughly similar width to the incisor of *E. obliquus* (Fig. 2o–q), but the two teeth display clearly distinct enamel microstructures (thick layer with Sbt. 3 *versus* thin layer with Sbt. 1–2 multiserial HSBs, respectively). If such a phylogenetic position for *Elasmodontomys* turns out to be correct, this taxon would thus represent the only case of an incisor enamel with a lower degree of resistance, among taxa that have all achieved the highest incisor enamel resistance (Sbt. 3 of multiserial HSBs) since the Paleogene. The acquisition of a Sbt. 1–2 of multiserial HSBs characterizing the incisor enamel of *Elasmodontomys* could then only be explained by a reversion toward this less resistant enamel condition from a very resistant one characterizing all octodontoids. From biomechanical and architectural perspectives, such a loss of three-dimensional enamel reinforcement is, however, hardly conceivable, since the selective pressure is rather towards strengthening the enamel of the heavily stressed incisor (T. Martin, pers. comm., which we follow). Given this unique case of enamel/phylogeny mismatch, an alternative would be to consider a possible sampling error regarding the extracted aDNA assumed to represent *Elasmodontomys* (after Woods et al. 2020), which could potentially be that of a hutia (capromyine), close to *Plagiodontia*, instead of *Elasmodontomys*. Without definitively calling into question the phylogenetic results of Woods et al. (2020) today, these puzzling incompatibilities then require that the aDNA extraction for *Elasmodontomys* to be duplicated, and new phylogenetic reconstructions to be performed (work in progress). *Elasmodontomys* still represents today a real morphological and phylogenetic *conundrum* as it displays primitive basicranial features that resemble “a wide variety of other taxa” (MacPhee 2011), inner ear traits intermediate between octodontoids and chinchilloids (i.e., Octochinchilloi; Da Cunha 2020, unpublished MSc results; Da Cunha et al., in prep.), some postcranial similarities with octodontoids (Patterson and Wood 1982; Woods and Hermanson 1985), an unusual chinchilloid cheek tooth laminar pattern characterized by a heterogeneous enamel layer (Marivaux et al. 2020), and an incisor enamel microstructure found in extinct

and extant chinchilloids, cavioids and erethizontoids, not in octodontoids (Martin 1992; this work).

Considering the phylogenetic significance of the incisor enamel microstructure (e.g., Korvenkontio 1934; Wahlert 1968; Boyde 1978; Koenigswald 1985; Martin 1992, 1993, 1994a, 1994b, 1997; Kalthoff 2000; Marivaux et al. 2004), it is clear for us that the different enamel patterns observed here among the West Indian caviomorphs indicate the presence of distinct high-level taxonomic groups. When crossed with morphological information deriving from dental and basicranial (middle and inner ears) anatomies, extinct and extant West Indian caviomorphs essentially document the Octochinchilloi (Octodontoidea and Chinchilloidea). The diversity of caviomorphs on the Caribbean islands is obviously the result of intra-archipelago diversification through time, but their high-level phylogenetic diversity can only be explained by distinct sources, implying *de facto* multiple natural colonizations of the West Indies. Recent gene-based phylogenies of extant Echimyidae, including West Indian Capromyinae (e.g., Fabre et al. 2014; Upham and Borroto-Páez 2017; Courcelle et al. 2019), are congruent for proposing a split of the insular forms from their South American relatives (*Carterodon*-like ancestor after Courcelle et al. 2019) sometime during the early/middle Miocene. The same is true when subfossil representatives of the West Indian capromyines and extinct heteropsomyines are included in these molecular data on extant Echimyidae (Woods et al. 2020). Capromyinae and Heteropsomyinae are resolved as sister taxa, thereby suggesting that their South American echimyid ancestor (i.e., *Carterodon*-like ancestor) most likely arrived in the Greater Antilles during a single dispersal event (Woods et al. 2020). Regarding the "heptaxodontid" chinchilloids (*Amblyrhiza*, *Clidomys*, and according to us *Elasmodontomys* and *Quemisia*), they most likely result from one (or several) separate dispersal event(s), staggered in time or perhaps concomitant with that of the echimyids. The question of one or multiple colonizations of the West Indies by South American chinchilloids, and the chronology of this or these dispersals, would require formally establishing the relative positions of the insular taxa in a comprehensive and dated phylogeny of Chinchilloidea (including all mainland taxa, i.e., extinct and extant dinomyids and chinchillids, and extinct neoepiblemids [and eventually extinct cephalomyids]). The recent discovery of a dinomyid chinchilloid (*Borikenomys praecursor*) in lower Oligocene deposits of Puerto Rico provides compelling evidence for an early dispersal of South American chinchilloids to the Caribbean islands near the Eocene/Oligocene transition (at the time of the GAARlandia land-bridge; Vélez-Juarbe et al. 2014; Marivaux et al. 2020 and references cited therein). With the fossil

dental material discovered, including incisors, we have re-analyzed here the incisor enamel microstructure of *Borikenomys* (formerly studied by Martin in Vélez-Juarbe et al. 2014), and noticed its strong microstructural similarities with the enamel condition characterizing Quaternary "heptaxodontids", in particular *Amblyrhiza* from the Anguilla Bank (Fig. 8). Similarly, this also suggest chinchilloid or “heptaxodontid” affinities for the late Oligocene unnamed taxon B described in Velez-Juarbe et al. (2014), also from Puerto Rico. Despite the limited fossil evidence currently assembled for *Borikenomys*, the unusual dental traits of the latter (e.g., laminae with heterogeneous thickness of the enamel layer, and narrow inter-lamina space filled with cement), which are otherwise retrieved only in several mainland chinchilloids (extinct and extant dinomyids and chinchillids) and in the West Indian[3] *Amblyrhiza*, *Elasmodontomys* and *Quemisia*, strongly suggest its possible phylogenetic link with these more recent chinchilloid forms of the islands (Marivaux et al. 2020). If this link is proven to be true, it would highlight the long-live insular lineage of the West Indian chinchilloids, including a tendency towards a spectacular island gigantism, as was achieved for some of their South American counterparts (e.g., Mones 1980; Sánchez-Villagra et al. 2003; Rinderknecht and Blanco 2008; Carrillo and Sánchez-Villagra 2015; Álvarez et al. 2017; Rinderknecht et al. 2018; Boivin et al. 2019c; Ferreira et al. 2020). “Giant hutias” unfortunately never reached modern times, although they potentially evolved on the islands for over 30 million years. Their possible long evolutionary history on the islands needs to be demonstrated/documented by paleontological data, especially for the Miocene epoch. It is in this sense that we are now concentrating our efforts in the field, in order to further document the fossil record of chinchilloids, but also of echimyid octodontoids (capromyines and heteropsomyines), as well as other island vertebrates (e.g., Blackburn et al. 2020; Marivaux et al. 2021; Viñola Lopez et al. 2022).

References

Alloing-Séguier L, Marivaux L, Barczi J-F, Lihoreau F, Martinand-Mari C (2019) Relationships between enamel prism decussation and behavior of the ameloblast layer in rodent incisors. Anat Rec 302:1195-1209. https://doi.org/10.1002/ar.24000

[3] The dental pattern of *Clidomys* is much more reminiscent to that of neoepiblemid chinchilloids (i.e., laminar pattern but without heterogeneity of the enamel layer).

Álvarez A, Arévalo RL, Verzi DH (2017) Diversification patterns and size evolution in caviomorph rodents. Biol J Linn Soc 121:907-922. https://doi.org/10.1093/biolinnean/blx026

Anthony HE (1916) Preliminary report of fossil mammals from Porto Rico, with descriptions of a new genus of ground sloth and two new genera of hystricomorph rodents. Ann N Y Acad Sci 27:193-203.

Anthony HE (1917) New fossil rodents from Porto Rico, with additional notes on *Elasmodontomys obliquus* Anthony and *Heteropsomys insulans* Anthony. Bull Am Mus Nat Hist 37:183-189.

Anthony HE (1918) The indigenous land mammals of Porto Rico, living and extinct. Mem Am Mus Nat Hist, new series 2:331-435.

Anthony HE (1920) New mammals from Jamaica. Bull Am Mus Nat Hist 42:469-475.

Anthony HE (1927) Mammals of Porto Rico, living and extinct - Rodentia and Edentata. Scientific Survey of Porto Rico and the Virgin Islands 9:97-155.

Antoine P-O, Marivaux L, Croft DA et al (2012) Middle Eocene rodents from Peruvian Amazonia reveal the pattern and timing of caviomorph origins and biogeography. Proc Roy Soc B 279:1319-1326. https://doi.org/10.1098/rspb.2011.1732

Antoine P-O, Abello MA, Adnet S et al (2016) A 60-million-year Cenozoic history of western Amazonian ecosystems in Contamana, eastern Peru. Gondwana Res 31:30-59. https://doi.org/10.1016/j.gr.2015.11.001

Antoine P-O, Yans J, Aliaga Castillo A et al (2021) Biotic community and landscape changes around the Eocene–Oligocene transition at Shapaja, Peruvian Amazonia: regional or global drivers? In: Hoorn C, Palazzesi L, Silvestro D (eds) Exploring the Impact of Andean Uplift and Climate on Life Evolution and Landscape Modification: from Amazonia to Patagonia. Glob Planet Change 202:103512. https://doi.org/10.1016/j.gloplacha.2021.103512

Arnal M, Kramarz AG, Vucetich MG, Vieytes EC (2014) A new early Miocene octodontoid rodent (Hystricognathi, Caviomorpha) from Patagonia (Argentina) and a reassessment of the early evolution of Octodontoidea. J Vert Paleontol 34:397-406. https://doi.org/10.1080/02724634.2013.808203

Assemat A, Boivin M, Marivaux L, Pujos F, Benites-Palomino A, Salas-Gismondi R, Tejada-Lara JV, Varas-Malca RM, Negri FR, Ribeiro AM, Antoine P-O (2019) Restes inédits de rongeurs caviomorphes du Paléogène de la région de Juanjui (Amazonie péruvienne) :

systématique, implications macro-évolutives et biostratigraphiques. Geodiversitas 41:699-730. https://doi.org/10.5252/geodiversitas2019v41a20

Biknevicius AR, McFarlane DA, MacPhee RDE (1993) Body size in *Amblyrhiza inundata* (Rodentia: Caviomorpha), an extinct megafaunal rodent from the Anguilla Bank, West Indies: estimates and implications. Am Mus Novitates 3079:1-25.

Blackburn DC, Keefe RM, Vallejo-Pareja MC, Vélez-Juarbe J (2020) The earliest record of Caribbean frogs: a fossil coquí from Puerto Rico. Biol Lett 16:20190947. https://doi.org/10.1098/rsbl.2019.0947

Boivin M, Marivaux L, Orliac MJ, Pujos F, Salas-Gismondi R, Tejada-Lara JV, Antoine P-O (2017) Late middle Eocene caviomorph rodents from Contamana, Peruvian Amazonia. Palaeontol Electron 50:1-50. https://doi.org/palaeo-electronica.org/content/2017/1822-eocene-amazonian-caviomorphs

Boivin M, Marivaux L, Antoine P-O (2019a) L'apport du registre paléogène d'Amazonie sur la diversification initiale des Caviomorpha (Hystricognathi, Rodentia) : implications phylogénétiques, macroévolutives et paléobiogéographiques. Geodiversitas 41:143-245. https://doi.org/10.5252/geodiversitas2019v41a4

Boivin M, Marivaux L, Salas-Gismondi R, Vieytes EC, Antoine P-O (2019b) Incisor enamel microstructure of Paleogene caviomorph rodents from Contamana and Shapaja (Peruvian Amazonia). J Mamm Evol 26:389-406. https://doi.org/10.1007/s10914-018-9430-4

Boivin M, Antoine P-O, Benites-Palomino A, Marivaux L, Salas-Gismondi R (2019c) A new record of a giant neoepiblemid rodent from Peruvian Amazonia and an overview of lower tooth dental homologies among chinchilloids. Acta Palaeontol Pol 64:627-642. https://doi.org/10.4202/app.00609.2019

Boivin M, Marivaux L, Aguirre-Díaz W et al (2022) Eocene caviomorph rodents from Balsayacu (Peruvian Amazonia). Paläontol Zeitsch 96:135-160. https://doi.org/10.1007/s12542-021-00551-0

Boyde A (1978) Development of the structure of the enamel of the incisor teeth in the three classical subordinal groups of the Rodentia. In: Butler PM, Josey KA (eds) Development, Function and Evolution of Teeth. Academic Press, London, pp 43-58.

Burgin CJ, Colella JP, Kahn PL, Upham NS (2018) How many species of mammals are there? J Mammal 99:1-14. https://doi.org/10.1093/jmammal/gyx147

Carrillo JD, Sánchez-Villagra MR (2015) Giant rodents from the Neotropics: diversity and dental variation of late Miocene neoepiblemid remains from Urumaco, Venezuela. Paläontol Zeitsch 89:1057-1071. https://doi.org/10.1007/s12542-015-0267-3

Cooke SB, Dávalos LM, Mychajliw AM, Turvey ST, Upham NS (2017) Anthropogenic extinction dominates Holocene declines of West Indian mammals. Annu Rev Ecol Evol Syst 48:301-327. https://doi.org/10.1146/annurev-ecolsys-110316-022754

Cope ED (1868) Exhibition of bones and teeth of a large rodent from the cave deposits of Anguilla, one of the Virgin West India Islands. Proc Acad Nat Sc Philadelphia 20:313.

Cope ED (1883) Contents of a bone cave in the island of Anguilla (West Indies). Smithsonian Contributions to Knowledge 25:1-30.

Courcelle M, Tilak M-K, Leite YLR, Douzery EJP, Fabre P-H (2019) Digging for the spiny rat and hutia phylogeny using a gene capture approach, with the description of a new mammal subfamily. Mol Phylogenet Evol 136:241-253. https://doi.org/10.1016/j.ympev.2019.03.007

Da Cunha L (2020) Oreille interne des rongeurs caviomorphes actuels et fossiles des Antilles : implications systématiques et phylogénétiques. Univ Montp Unpub MSc research internship.

Dávalos LM (2004) Phylogeny and biogeography of Caribbean mammals. Biol J Linn Soc 81:373-394. https://doi.org/10.1111/j.1095-8312.2003.00302.x

Fabre P-H, Vilstrup JT, Raghavan M, Der Sarkissian C, Willerslev E, Douzery EJP, Orlando L (2014) Rodents of the Caribbean: origin and diversification of hutias unravelled by next-generation museomics. Biol Lett 10:20140266. https://doi.org/10.1098/rsbl.2014.0266

Fabre P-H, Hautier L, Douzery EJP (2015) A synopsis of rodent molecular phylogenetics, systematics and biogeography. In: Cox PG, Hautier L (eds) Evolution of the Rodents: Advances in Phylogeny, Functional Morphology and Development. Cambridge University Press, Cambridge, pp 19-69.

Ferreira JD, Negri FR, Sánchez-Villagra MR, Kerber L (2020) Small within the largest: brain size and anatomy of the extinct *Neoepiblema acreensis*, a giant rodent from the Neotropics. Biol Lett 16:20190914. https://doi.org/10.1098/rsbl.2019.0914

Ginot S, Hautier L, Marivaux L, Vianey-Liaud M (2016) Ecomorphological analysis of the astragalo-calcaneal complex in rodents and inferences of locomotor behaviours in extinct rodent species. PeerJ 4:1-49. https://doi.org/10.7717/peerj.2393

Hedges SB (2006) Paleogeography of the Antilles and origin of West Indian terrestrial vertebrates. Ann Missouri Bot Gard 93:231-244.

Kalthoff D (2000) Die Schmelzmikrostruktur in den incisiven der hamsterartigen Nagetiere und anderer Myomorpha (Rodentia, Mammalia). Palaeontogr A 259:1-193.

Kerber L, Negri FR, Ribeiro AM, Nasif N, Pereira de Souza-Filho J, Ferigolo J (2017) Tropical fossil caviomorph rodents from the southwestern Brazilian Amazonia in the context of the South American faunas: systematics, biochronology, and paleobiogeography. J Mamm Evol 24:57-70. https://doi.org/10.1007/s10914-016-9340-2

Kerber L, Bissaro Junior MC, Negri FR, Pereira de Souza-Filho J, Guilherme E, Schmaltz Hsiou A (2018) A new rodent (Caviomorpha: Dinomyidae) from the upper Miocene of southwestern Brazilian Amazonia. Hist Biol 30:985-993. https://doi.org/10.1080/08912963.2017.1327529

Kerber L, Negri FR, Sanfelice D (2019) Morphology of cheek teeth and dental replacement in the extinct rodent *Neoepiblema* Ameghino, 1889 (Caviomorpha, Chinchilloidea, Neoepiblemidae). J Vert Paleontol 38:e1549061. https://doi.org/10.1080/02724634.2018.1549061

Koenigswald W v (1985) Evolutionary trends in the enamel of rodent incisors. In: Luckett WP, Hartenberger J-L (eds) Evolutionary Relationships among Rodents, A Multidisciplinary Analysis. Plenum, New York, pp 403-422.

Koenigswald W v, Sander PM (1997) Glossary of terms used for enamel microstructures. In: Koenigswald W v, Sander PM (eds) Tooth Enamel Microstructure. Balkema, Rotterdam, pp 267-280.

Korvenkontio VA (1934) Mikroskopische Untersuchungen an Nagerincisiven unter Hinweis auf die Schmelzstruktur der Backenzähne. Ann Zoo Soc Zool – Bota Fennicae Vanamo 2:1-274.

Kramarz AG, Vucetich MG, Arnal M (2013) A new Early Miocene chinchilloid hystricognath rodent. An approach to the understanding of the early chinchillid dental evolution. J Mamm Evol 20:249-261. https://doi.org/10.1007/s10914-012-9215-0

MacPhee RDE (1984) Quaternary mammal localities and heptaxodontid rodents of Jamaica. Am Mus Novitates 2803:1-34.

MacPhee RDE (2009) *Insulae infortunatae*: establishing a chronology for Late Quaternary mammal extinctions in the West Indies. In: Haynes G (ed) American Megafaunal Extinctions at the End of the Pleistocene. Springer, Dordrecht, pp 169-193.

MacPhee RDE (2011) Basicranial morphology and relationships of Antillean Heptaxodontidae (Rodentia, Ctenohystrica, Caviomorpha). Bull Am Mus Nat Hist 363:1-70.

MacPhee RDE, Flemming C (2003) A possible heptaxodontine and other caviidan rodents from the Quaternary of Jamaica. Am Mus Novitates 3422:1-42.

MacPhee RDE, Iturralde-Vinent MA (1995) Origin of the Greater Antillean land mammal fauna, 1: new Tertiary fossils from Cuba and Puerto Rico. Am Mus Novitates 3141:1-30.

MacPhee RDE, Iturralde-Vinent MA (2005) The interpretation of Caribbean paleogeography: reply to Hedges. In Alcover JA, Bover P (eds), Proceedings of the International Symposium on Insular Vertebrate Evolution: the Palaeontological Approach. Monograf Soc Hist Nat Balears, pp 175-184.

MacPhee RDE, Iturralde-Vinent MA, Gaffney ES (2003) Domo de Zaza, an early Miocene vertebrate locality in South-Central Cuba, with notes on the tectonic evolution of Puerto Rico and the Mona passage. Am Mus Novitates 3394:1-42.

Mares MA, Ojeda A (1982) Patterns of diversity and adaptation in South American hystricognath rodents. In: Mares MA, Genoways HH (eds) Mammalian Biology in South America. Pymatuning Laboratory of Ecology, Pittsburgh, pp 185-192.

Marivaux L, Vianey-Liaud M, Jaeger J-J (2004) High-level phylogeny of early Tertiary rodents: dental evidence. Zool J Linn Soc 142:105-134. https://doi.org/10.1111/j.1096-3642.2004.00131.x

Marivaux L, Boivin M, Adnet S, Benammi M, Tabuce R, Benammi M (2019) Incisor enamel microstructure of hystricognathous and anomaluroid rodents from the earliest Oligocene of Dakhla, Atlantic Sahara (Morocco). J Mamm Evol 26:373-388. https://doi.org/10.1007/s10914-017-9426-5

Marivaux L, Vélez-Juarbe J, Merzeraud G et al (2020) Early Oligocene chinchilloid caviomorphs from Puerto Rico and the initial rodent colonization of the West Indies. Proc Roy Soc B 287:20192806. https://doi.org/10.1098/rspb.2019.2806

Marivaux L, Vélez-Juarbe J, Viñola López LW et al (2021) An unpredicted ancient colonization of the West Indies by North American rodents: dental evidence of a geomorph from the early Oligocene of Puerto Rico. Pap Palaeontol 7:2021-2039. https://doi.org/10.1002/spp2.1388

Martin T (1992) Schmelzmikrostruktur in den inzisiven alt-und neuweltlicher hystricognather Nagetiere. Palaeovertebrata Mém extra:1-168.

Martin T (1993) Early rodent incisor enamel evolution: phylogenetic implications. J Mamm Evol 1:227-254. https://doi.org/10.1007/BF01041665

Martin T (1994a) African origin of caviomorph rodents is indicated by incisor enamel microstructure. Paleobiology 20:5-13. https://doi.org/10.1017/S009483730001109X

Martin T (1994b) On the systematic position of *Chaetomys subspinosus* (Rodentia: Caviomorpha) based on evidence from the incisor enamel microstructure. J Mamm Evol 2:117-131. https://doi.org/10.1007/BF01464364

Martin T (1997) Incisor enamel microstructure and systematics in rodents. In: Koenigswald W von, Sander PM (eds) Tooth Enamel Microstructure. Balkema, Rotterdam, pp 163-175.

Martin T (2004) Incisor enamel microstructure of South America's earliest rodents: implications for caviomorph origin and diversification. In: Campbell KE (ed) The Paleogene Mammalian Fauna of Santa Rosa, Amazonian Peru. Nat Hist Mus Los Angeles County, Los Angeles, pp 131-140.

Martin T (2005) Incisor schmelzmuster diversity in South America's oldest rodent fauna and early caviomorph history. J Mamm Evol 12:405-417. https://doi.org/10.1007/s10914-005-6968-8

McKenna MC, Bell SK (1997) Classification of Mammals Above the Species Level. Columbia University Press, New York.

Miller GS (1929) Mammals eaten by Indians, owls, and spaniards in the coast region of the Dominican Republic. Smithsonian Misc Collect 82:1-16.

Miller GS, Gidley JW (1918) Synopsis of the supergeneric groups of rodents. J Wash Acad Sci 8:431-448.

Mones A (1980) Un Neoepiblemidae del Plioceno medio (Formacion Urumaco) de Venezuela (Mammalia: Rodentia: Caviomorpha). Ameghiniana 17:277-279.

Morgan GS, Wilkins L (2003) The extinct rodent *Clidomys* (Heptaxodontidae) from a late Quaternary cave deposit in Jamaica. Caribb J Earth Sci 39:34-41.

Orihuela J, Viñola LW, Jiménez Vázquez O, Mychajliw AM, Hernández de Lara O, Lorenzo L, Soto-Centeno JA (2020) Assessing the role of humans in Greater Antillean land vertebrate extinctions: new insights from Cuba. Quat Sci Rev 249:106597. https://doi.org/10.1016/j.quascirev.2020.106597

Patterson B, Wood AE (1982) Rodents from the Deseadan Oligocene of Bolivia and the relationship of Caviomorpha. Bull Mus Comp Zool 149:372-543.

Patton JL, Pardiñas UF, d'Elia G (2015) Mammals of South America. Vol. 2: Rodents. University of Chicago Press, Chicago.

Rasia LL, Candela AM, Cañon C (2021) Comprehensive total evidence phylogeny of chinchillids (Rodentia, Caviomorpha): cheek teeth anatomy and evolution. J Anat 239:405-423. https://doi.org/10.1111/joa.13430

Ray CE (1965) The relationships of Quemisia gravis (Rodentia: ?Heptaxodontidae). Smithsonian Misc Collect 149:1-12.

Rinderknecht A, Blanco RE (2008) The largest fossil rodent. Proc Roy Soc B 275:923-928. https://doi.org/10.1098/rspb.2007.1645

Rinderknecht A, Bostelmann E, Ubilla M (2018) Making a giant rodent: cranial anatomy and ontogenetic development in the genus *Isostylomys* (Mammalia, Hystricognathi, Dinomyidae). J Syst Palaeontol 16:245-261. https://doi.org/10.1080/14772019.2017.1285360

Robinet C, Merceron G, Candela AM, Marivaux L (2020) Dental microwear texture analysis and diet in extant caviomorphs (Rodentia) from the Serra do Mar Atlantic forest ecoregion (Brazil). J Mammal 101:386-402. https://doi.org/10.1093/jmammal/gyz194

Robinet C, Merceron G, Catzeflis F, Candela AM, Marivaux L (2022) About inter- and intra-specific variability of dental microwear texture in rodents: study of two sympatric *Proechimys* (Echimyidae) species from the Cacao locality, French Guiana. In: Merceron G, Tutken T, Scott R (eds) Understanding Dental Proxies of Ancient Diets. Palaeogeogr Palaeoclimatol Palaeoecol 591:110880. https://doi.org/10.1016/j.palaeo.2022.110880

Sánchez-Villagra MR, Aguilera O, Horovitz I (2003) The anatomy of the world's largest extinct rodent. Science 301:1708-1710. https://doi.org/10.1126/science.1089332

Schreuder A (1933) Skull of *Amblyrhiza* from St. Martin. Tijdschr Nederl Dierk Vereening 3:242-266.

Simpson GG (1945) The principles of classification and a classification of mammals. Bull Am Mus Nat Hist 85:1-350.

Townsend KEB, Croft DA (2008) Enamel microwear in caviomorph rodents. J Mammal 89:730-743.

Turvey ST, Grady FV, Rye P (2006) A new genus and species of 'giant hutia' (*Tainotherium valei*) from the Quaternary of Puerto Rico: an extinct arboreal quadruped? J Zool 270:585-594. https://doi.org/10.1111/j.1469-7998.2006.00170.x

Turvey ST, Kennerley RJ, Nuñez-Miño JM, Young RP (2017) The Last Survivors: current status and conservation of the non-volant land mammals of the insular Caribbean. J Mammal 98:918-936. https://doi.org/10.1093/jmammal/gyw154

Upham NS, Borroto-Páez R (2017) Molecular phylogeography of endangered Cuban hutias within the Caribbean radiation of capromyid rodents. J Mammal 98:950-963. https://doi.org/10.1093/jmammal/gyx077

Upham NS, Patterson BD (2015) Evolution of caviomorph rodents: a complete phylogeny and timetree for living genera. In: Vassallo AI, Antenucci D (eds) Biology of Caviomorph Rodents: Diversity and Evolution. SAREM Series A, Buenos Aires, pp 63-120.

Vélez-Juarbe J, Martin T, MacPhee RDE, Ortega-Ariza D (2014) The earliest Caribbean rodents: Oligocene caviomorphs from Puerto Rico. J Vert Paleontol 34:157-163. https://doi.org/10.1080/02724634.2013.789039

Vieytes EC, Morgan CC, Verzi DH (2007) Adaptive diversity of incisor enamel microstructure in South American burrowing rodents (family Ctenomyidae, Caviomorpha). J Anat 211:296-302. https://doi.org/10.1111/j.1469-7580.2007.00767.x

Viñola López LW, Core Suárez EE, Vélez-Juarbe J, Almonte Milan JN, Bloch JI (2022) The oldest known record of a ground sloth (Mammalia, Xenarthra, Folivora) from Hispaniola: evolutionary and paleobiogeographical implications. J Paleontol 96: 684-691. https://doi.org/10.1017/jpa.2021.109

Vucetich MG, Vieytes EC (2006) A middle Miocene primitive octodontoid rodent and its bearing on the early evolutionary history of the Octodontoidea. Palaeontogr Abt A 277:81–91. https://doi.org/10.1127/pala/277/2006/81

Vucetich MG, Kramarz AG, Candela AM (2010) Colhuehuapian rodents from Gran Barranca and other Patagonian localities: the state of the art. In: Madden RH, Carlini AA, Vucetich MG, Kay RF (eds) The Paleontology of Gran Barranca: Evolution and Environmental Change through the Middle Cenozoic of Patagonia. Cambridge University Press, New York, pp 206-219.

Vucetich MG, Arnal M, Deschamps CM, Pérez ME, Vieytes EC (2015) A brief history of caviomorph rodents as told by the fossil record. In: Vassallo AI, Antenucci D (eds) Biology of Caviomorph Rodents: Diversity and Evolution. SAREM Series A, Buenos Aires, pp 11-62.

Wahlert JH (1968) Variability of rodent incisor enamel as viewed in thin section, and the microstructure of the enamel in fossil and Recent rodent groups. Breviora, Mus Comp Zool 309:1-18.

Wilson DE, Reeder DM (2005) Mammal Species of the World: a Taxonomic and Geographic Reference. Johns Hopkins University Press, Baltimore.

Wilson DE, Lacher TE, Mittermeier RA (2016) Handbook of the Mammals of the World. Vol. 6. Lagomorphs and Rodents. Lynx Edicions, Barcelona.

Wilson LAB, Geiger M (2015) Diversity and evolution of femoral variation in Ctenohystrica. In: Cox PG, Hautier L (eds) Evolution of the Rodents: Advances in Phylogeny,

Functional Morphology and Development. Cambridge University Press, Cambridge, pp 510-538.

Woods CA (1989) The biogeography of West Indian rodents. In: Woods CA (ed) Biogeography of the West Indies; Past, Present, and Future. Sandhill Crane, Gainesville, pp 741-798.

Woods CA, Hermanson JW (1985) Myology of hystricognath rodents: an analysis of form, function and phylogeny. In: Luckett PW, Hartenberger J-L (eds) Evolutionary Relationships Among Rodents: a Multidisciplinary Analysis. Plenum, New York, pp 515-548.

Woods CA, Borroto-Páez R, Kilpatrick CW (2001) Insular patterns and radiations of West Indian rodents. In: Woods CA, Sergile FE (eds) Biogeography of the West Indies: Patterns and Perspectives. CRC Press, Boca Raton, pp 335-353.

Woods R, Barnes I, Brace S, Turvey ST (2020) Ancient DNA suggests single colonisation and within-archipelago diversification of Caribbean caviomorph rodents. Mol Biol Evol 38:84-95. https://doi.org/10.1093/molbev/msaa189

Figure captions

Fig. 1 Optical and scanning electron photomicrographs of an incisor for which the enamel microstructure is revealed in section after polishing and etching. **a.** longitudinal section of the incisor (here *Capromys pilorides*) showing the enamel layer on the buccal aspect of the tooth (optical incident light photography); **b.** studied area of the enamel layer at higher magnification, showing inclined Hunter-Schreger bands (HSBs) (optical incident light photography); **c.** studied area of the enamel layer, revealing microstructural details (scanning electron photomicrograph): the *portio externa* (PE) is the outer part of the enamel layer, displaying radial enamel, whereas the *portio interna* (PI), generally representing the largest proportion (%) of the total enamel thickness, displays multiserial HSBs. On this given sample, HSBs are inclined at ~35° to the enamel-dentine junction (EDJ); **d.** microstructural detail of '**c**' showing seven decussating HSBs with five to six prisms per band, and the crystallites of the inter-prismatic matrix (IPM) forming thin plates between the prism rows (inter-row sheets) that run perpendicular to the prism long axes (direction), without any anastomosis between prisms

Fig. 2 Incisor cross-sections of sampled hystricognathous rodents from the West Indies and South America. Most of specimens from the West Indies are subfossils (see Table 1). **a.** UF 520141, *Isolobodon portoricensis*; **b.** UF 333712, *Isolobodon montanus*; **c.** UF 520143, *Hexolobodon phenax*; **d.** UF 70850, *Rhizoplagiodontia lemkei*; **e.** UF 520142, *Plagiodontia ipnaeum*; **f.** UF 5201444, *Capromys pilorides*; **g.** *Geocapromys caymanensis*; **h.** CLV 2595, *Geocapromys columbianus*; **i.** CLV 401, *Macrocapromys acevedo*; **j.** CLV 2597, *Mesocapromys nanus*; **k.** UF 333716, *Brotomys contractus*; **l.** CVL 2596, *Boromys offella*; **m.** CLV 2598, *Boromys torrei*; **n.** UPRMP-3229, *Heteropsomys* sp.; **o.** UPRMP-3230, *Elasmodontomys obliquus*; **p.** UPRMP-3231, *Elasmodontomys obliquus*; **q.** UPRMP-3232, *Elasmodontomys obliquus*; **r.** UF 274295, *Clidomys* sp.; **s.** UM-SB-Coco-03, *Amblyrhiza* sp.; **t.** UM-SB-Coco-04, *Amblyrhiza* sp. (juvenile); **u.** LACM 162956, *Borikenomys praecursor*; **v.** UM 524N, *Mysateles* sp.; **w.** UM N385, *Cuniculus paca*; **x.** UM 521N, *Lagidium* sp.; **y.** UM N312, *Chinchilla* sp. Some of specimens have the dentine dammaged (dashed lines). **a**–**d**, **h**–**j**, **l**, **n**–**q** and **s**–**y**: lower incisors. **e**–**g**, **k** and **m**: upper incisors. **r**, lower or upper incisor. Scale bar equals 1 mm

Fig. 3 Scanning electron photomicrographs of incisors of subfossil spiny rat hutias (Echimyidae Capromyinae) from the West Indies, for which the enamel microstructure (multiserial HSBs) is shown in longitudinal section and at different magnifications. The left pictures illustrate an overview of the enamel layer for each specimen, and the associated right ones a detail of the microstructure in PI. **a**–**b.** *Isolobodon portoricensis* (UF 520141); **c**–**d.** *Isolobodon montanus* (UF 333172); **e**–**f.** *Hexolobodon phenax* (UF 520143, reversed); **g**–**h.** *Rhizoplagiodontia lemkei* (UF 70850)

Fig. 4 Scanning electron photomicrographs of incisors of subfossil spiny rat hutias (Echimyidae Capromyinae) from the West Indies, for which the enamel microstructure (multiserial HSBs) is shown in longitudinal section and at different magnifications. The left pictures illustrate an overview of the enamel layer for each specimen, and the associated right ones a detail of the microstructure in PI. **a**–**b.** *Plagiodontia ipnaeum* (UF 520142); **c**–**d.** *Capromys pilorides lewisi* (UF 520144); **e**–**f.** *Geocapromys caymanensis* (UF 520145); **g**–**h.** *Geocapromys columbianus* (CLV 2595, reversed)

Fig. 5 Scanning electron photomicrographs of incisors of subfossil and extant spiny rat hutias (Echimyidae Capromyinae) from the West Indies, for which the enamel microstructure (multiserial HSBs) is shown in longitudinal section and at different magnifications. The left pictures illustrate an overview of the enamel layer for each specimen, and the associated right ones a detail of the microstructure in PI. **a**–**b.** *Macrocapromys acedo* (CVL 401, reversed); **c**–**d.** *Mesocapromys nanus* (UF 520144); **e**–**f.** *Mysateles* sp. (UM 524N, reversed)

Fig. 6 Scanning electron photomicrographs of incisors of subfossil spiny rats (Echimyidae Heteropsomyinae) from the West Indies, for which the enamel microstructure (multiserial HSBs) is shown in longitudinal section and at different magnifications. The left pictures illustrate an overview of the enamel layer for each specimen, and the associated right ones a detail of the microstructure in PI. **a**–**b.** *Brotomys contractus* (UF 333716, reversed); **c**–**d.** *Boromys offella* (CLV 2596); **e**–**f.** *Boromys torrei* (CLV 2598); **g**–**h.** *Heteropsomys* sp. (UPRMP-3229, reversed)

Fig. 7 Scanning electron photomicrographs of incisors of subfossil giant hutias *Elasmodontomys* and *Clidomys* from Puerto Rico and Jamaica, respectively, for which the enamel microstructure (multiserial HSBs) is shown in longitudinal section and at different magnifications. The left pictures illustrate an overview of the enamel layer for each specimen, and the associated right ones a detail of the microstructure in PI. **a**–**b.** *Elasmodontomys obliquus* (UPRMP-3230); **c**–**d.** *Elasmodontomys obliquus* (UPRMP-3231); **e**–**f.** *Elasmodontomys obliquus* (UPRMP-3232); **g**–**h.** *Clidomys* sp. (UF 274295)

Fig. 8 Scanning electron photomicrographs of incisors of the subfossil giant hutias *Amblyrhiza* from St. Barth, and of the chinchilloid *Borikenomys* from the early Oligocene of Puerto Rico, for which the enamel microstructure (multiserial HSBs) is shown in longitudinal section and at different magnifications (overview of the enamel layer and details of the microstructure in PI). **a**–**d.** *Amblyrhiza* sp. (UM SB-Coco-03); **e**–**f.** *Amblyrhiza* sp. (juvenile; UM SB-Coco-04); **g**–**h.** *Borikenomys praecursor* (LACM 162956)

Fig. 9 Scanning electron photomicrographs of incisors of extant caviomorph rodents (Chinchillidae Chinchilloidea and Cuniculidae Cavioidea) from South America, for which the enamel microstructure (multiserial HSBs) is shown in longitudinal section and at different magnifications. The left pictures illustrate an overview of the enamel layer for each specimen, and the associated right ones a detail of the microstructure in PI. **a**–**b.** *Lagidium* sp. (UM 521N, reversed); **c**–**d.** *Chinchilla* sp. (UM N312, reversed); **e**–**f.** *Cuniculus paca* (UM N385)

Table captions

Table 1 List of sampled taxa for incisor enamel microstructure analyses with indications on their geographic provenance, age and collectors/collections. Abbreviations: CLV, *Colección Lazaro Viñola*; Coll., Collection; FMNH, Florida Museum of Natural History, Division of Vertebrate Paleontology, USA; LACM, Natural History Museum of Los Angeles County, USA; SB, Saint-Barthélemy, French West Indies; UF, University of Florida, USA; UM, *Université de Montpellier*, France; UPRMP, University of Puerto Rico, Mayaguez (Paleontology Collection, Department of Geology), Puerto Rico, USA; (frag.) means fragment of incisor. The date format used here is DD/MM/YY

Table 2 Enamel characters and measurements of the studied incisor specimens. All incisor sections display multiserial HSBs. Enamel distinctions are made between some incisors depending on the arrangement and direction of the hydroxyapatite crystallites of the IPM, with respect to the crystallites of the prisms, thereby describing different subtypes (Sbt.) or transitional subtypes of multiserial enamel. Arbitrary division of the range of the angle (α) formed between the IPM crystallites and the prism crystallites: parallel to very low acute angle ($0° \leq \alpha \leq 15°$); low acute angle ($15° < \alpha \leq 40°$); medium to high acute angle ($40° < \alpha \leq 70°$); very high acute to right angle ($70° < \alpha \leq 90°$). Abbreviations: HSB, Hunter-Schreger band; IPM, inter-prismatic matrix; mm, millimeters; PE, *portio externa*; PI, *portio interna*; †, extinct; #, slightly different from

Supplementary Material

Online Resource 1 Incisor enamel microstructure for extant and extinct Ctenohystrica

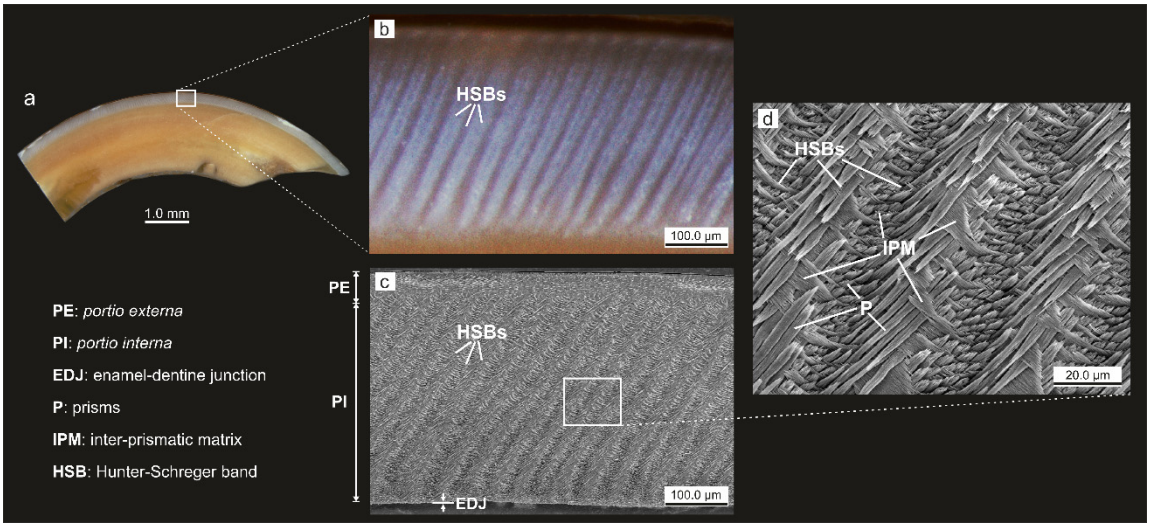

Fig. 1 Optical and scanning electron photomicrographs of an incisor for which the enamel microstructure is revealed in section after polishing and etching. **a** longitudinal section of the incisor (here *Capromys pilorides*) showing the enamel layer on the labial aspect of the tooth (optical incident light photography); **b** studied area of the enamel layer at higher magnification, showing inclined Hunter-Schreger bands (HSBs) (optical incident light photography); **c** studied area of the enamel layer, revealing microstructural details (scanning electron photomicrograph): the *portio externa* (PE) is the outer part of the enamel layer, displaying radial enamel, whereas the *portio interna* (PI), generally representing the largest proportion (%) of the total enamel thickness, displays multiserial HSBs. On this given sample, HSBs are inclined at ~35° to the enamel-dentine junction (EDJ); **d** microstructural detail of 'c' showing seven decussating HSBs with five to six prisms per band, and the crystallites of the inter-prismatic matrix (IPM) forming thin plates between the prism rows (inter-row sheets) that run perpendicular to the prism long axes (direction), without any anastomosis between prisms

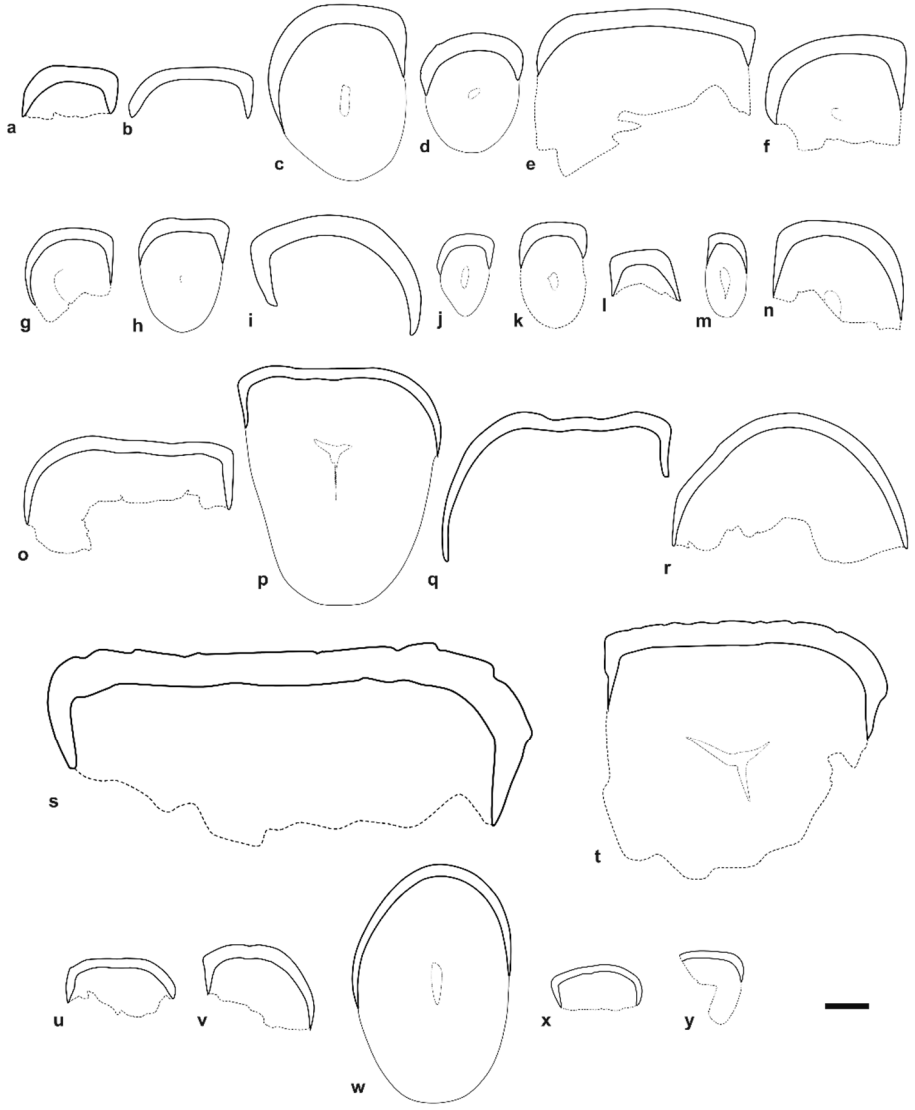

Fig. 2 Incisor cross-sections of sampled hystricognathous rodents from the West Indies and South America. Most of specimens from the West Indies are subfossils (see Table 1). **a** UF 520141, *Isolobodon portoricensis*; **b** UF 333712, *Isolobodon montanus*; **c** UF 520143, *Hexolobodon phenax*; **d** UF 70850, *Rhizoplagiodontia lemkei*; **e** UF 520142, *Plagiodontia ipnaeum*; **f** UF 520144, *Capromys pilorides*; **g** *Geocapromys caymanensis*; **h** CLV 2595, *Geocapromys columbianus*; **i** CLV 401, *Macrocapromys acevedo*; **j** CLV 2597, *Mesocapromys nanus*; **k** UF 333716, *Brotomys contractus*; **l** CVL 2596, *Boromys offella*; **m** CLV 2598, *Boromys torrei*; **n** UPRMP-3229, *Heteropsomys* sp.; **o** UPRMP-3230, *Elasmodontomys obliquus*; **p** UPRMP-3231, *Elasmodontomys obliquus*; **q** UPRMP-3232, *Elasmodontomys obliquus*; **r** UF 274295, *Clidomys* sp.; **s** UM SB-Coco-03, *Amblyrhiza* sp.; **t** UM SB-Coco-04, *Amblyrhiza* sp. (juvenile); **u** LACM 162956, *Borikenomys praecursor*; **v** UM 524N, *Mysateles* sp.; **w** UM N385, *Cuniculus paca*; **x** UM 521N, *Lagidium* sp.; **y** UM N312, *Chinchilla* sp. Some of specimens have the dentine dammaged (dashed lines). a–d, h–j, l, n–q and s–y: lower incisors. e–g, k and m: upper incisors. r, lower or upper incisor. Scale bar = 1 mm

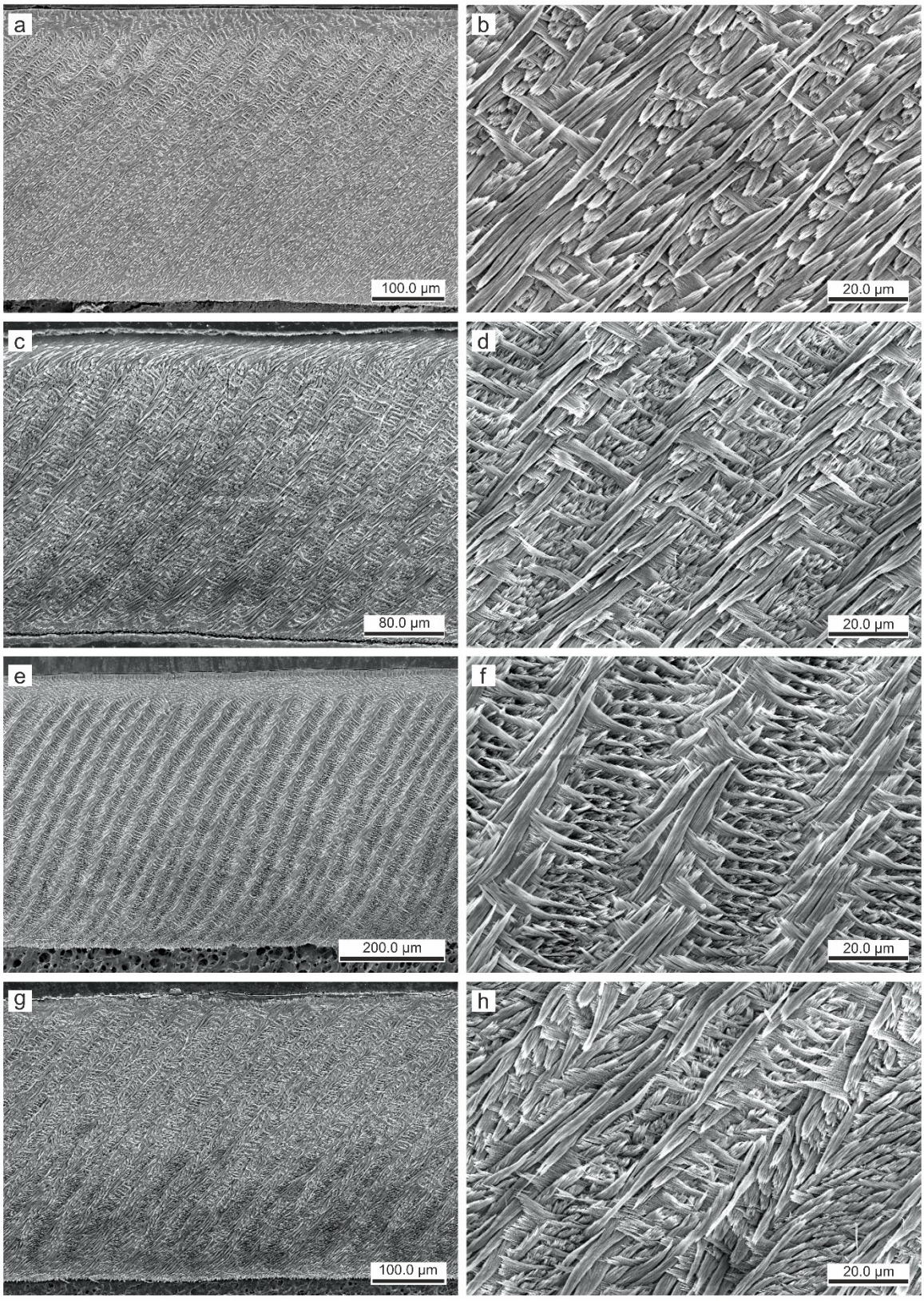

Fig. 3 Scanning electron photomicrographs of incisors of subfossil spiny rat hutias (Echimyidae Capromyinae) from the West Indies, for which the enamel microstructure (multiserial HSBs) is shown in longitudinal section and at different magnifications. The left pictures illustrate an overview of the enamel layer for each specimen, and the associated right ones a detail of the microstructure in PI. **a–b** *Isolobodon portoricensis* (UF 520141); **c–d** *Isolobodon montanus* (UF 333172); **e–f** *Hexolobodon phenax* (UF 520143, reversed); **g–h** *Rhizoplagiodontia lemkei* (UF 70850)

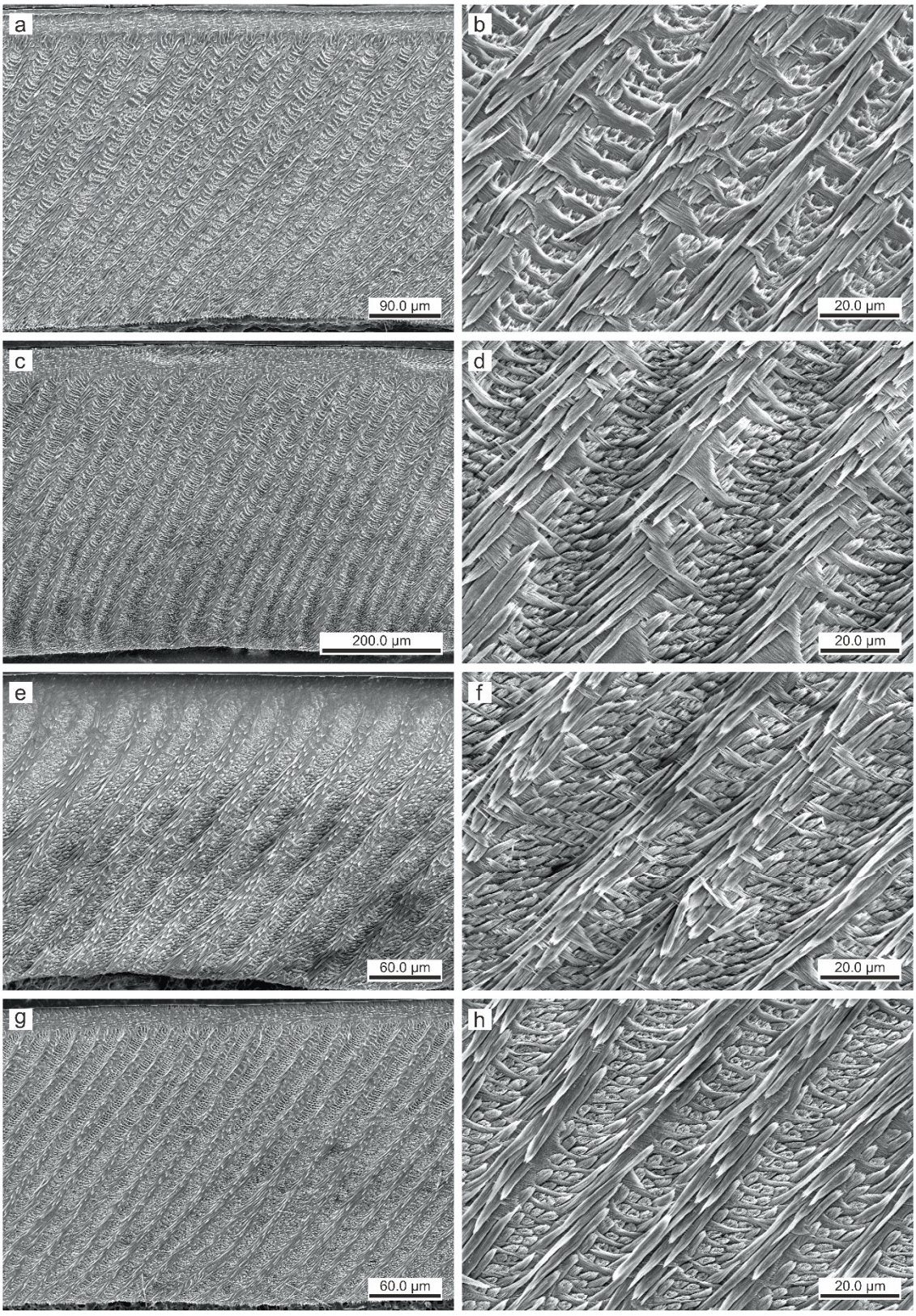

Fig. 4 Scanning electron photomicrographs of incisors of subfossil spiny rat hutias (Echimyidae Capromyinae) from the West Indies, for which the enamel microstructure (multiserial HSBs) is shown in longitudinal section and at different magnifications. The left pictures illustrate an overview of the enamel layer for each specimen, and the associated right ones a detail of the microstructure in PI. **a–b** *Plagiodontia ipnaeum* (UF 520142); **c–d** *Capromys pilorides lewisi* (UF 520144); **e–f** *Geocapromys caymanensis* (UF 520145); **g–h** *Geocapromys columbianus* (CLV 2595, reversed)

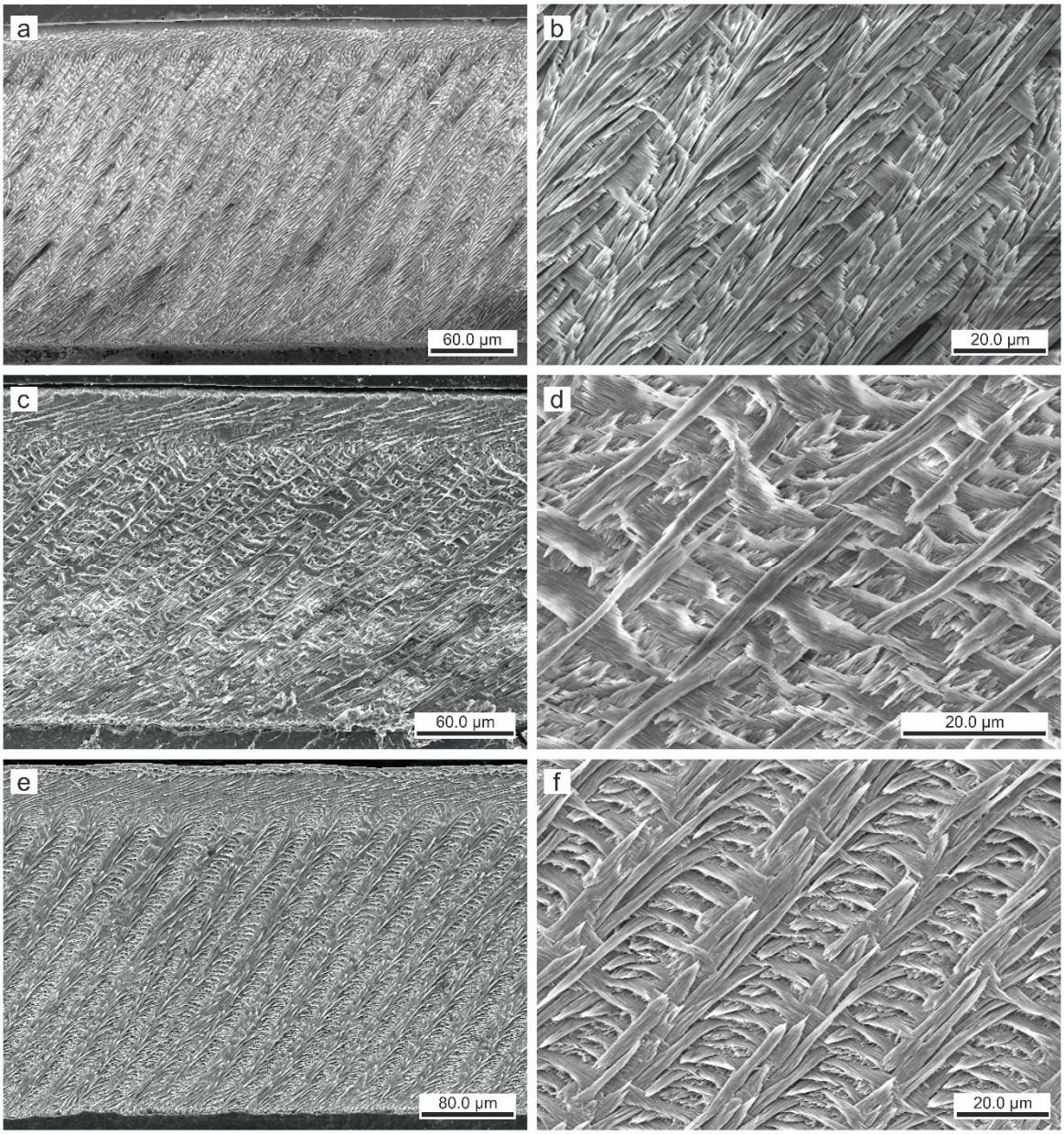

Fig. 5 Scanning electron photomicrographs of incisors of subfossil and extant spiny rat hutias (Echimyidae Capromyinae) from the West Indies, for which the enamel microstructure (multiserial HSBs) is shown in longitudinal section and at different magnifications. The left pictures illustrate an overview of the enamel layer for each specimen, and the associated right ones a detail of the microstructure in PI. **a–b** *Macrocapromys acedo* (CVL 401, reversed); **c–d** *Mesocapromys nanus* (UF 520144); **e–f** *Mysateles* sp. (UM 524N, reversed)

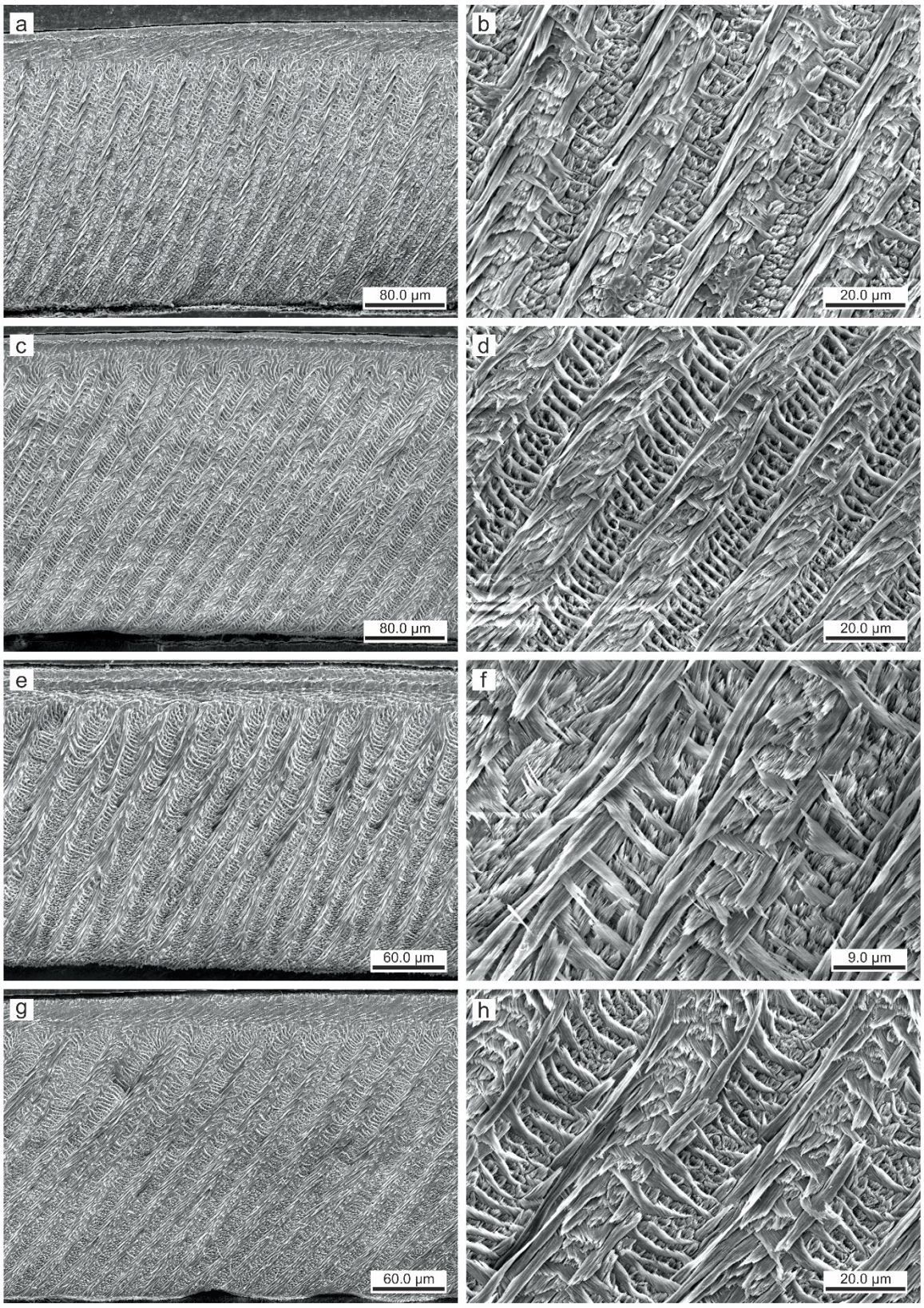

Fig. 6 Scanning electron photomicrographs of incisors of subfossil spiny rats (Echimyidae Heteropsomyinae) from the West Indies, for which the enamel microstructure (multiserial HSBs) is shown in longitudinal section and at different magnifications. The left pictures illustrate an overview of the enamel layer for each specimen, and the associated right ones a detail of the microstructure in PI. **a–b** *Brotomys contractus* (UF 333716, reversed); **c–d** *Boromys offella* (CLV 2596); **e–f** *Boromys torrei* (CLV 2598); **g–h** *Heteropsomys* sp. (UPRMP-3229, reversed)

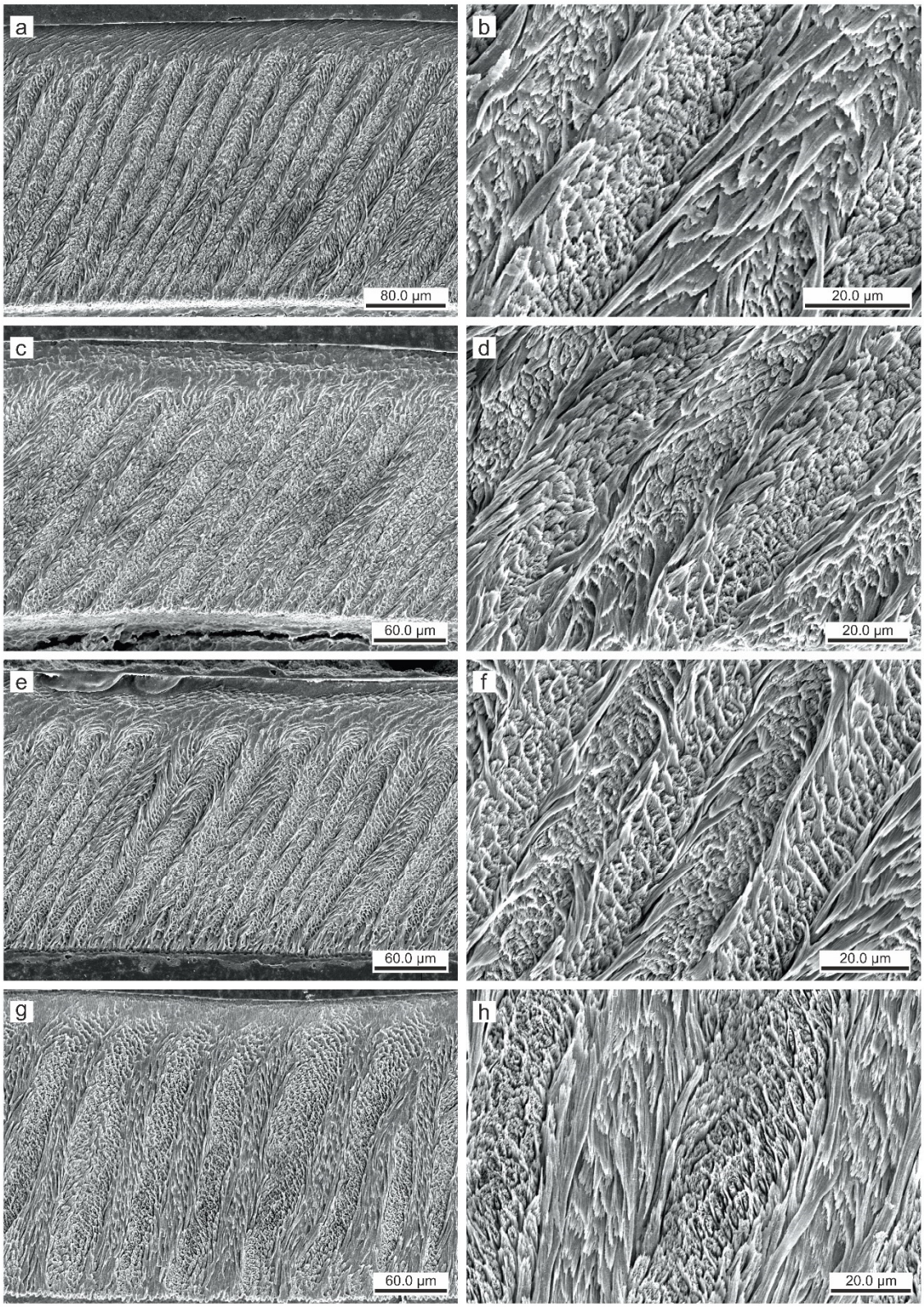

Fig. 7 Scanning electron photomicrographs of incisors of subfossil giant hutias *Elasmodontomys* and *Clidomys* from Puerto Rico and Jamaica, respectively, for which the enamel microstructure (multiserial HSBs) is shown in longitudinal section and at different magnifications. The left pictures illustrate an overview of the enamel layer for each specimen, and the associated right ones a detail of the microstructure in PI. **a–b** *Elasmodontomys obliquus* (UPRMP-3230); **c–d** *Elasmodontomys obliquus* (UPRMP-3231); **e–f** *Elasmodontomys obliquus* (UPRMP-3232); **g–h** *Clidomys* sp. (UF 274295)

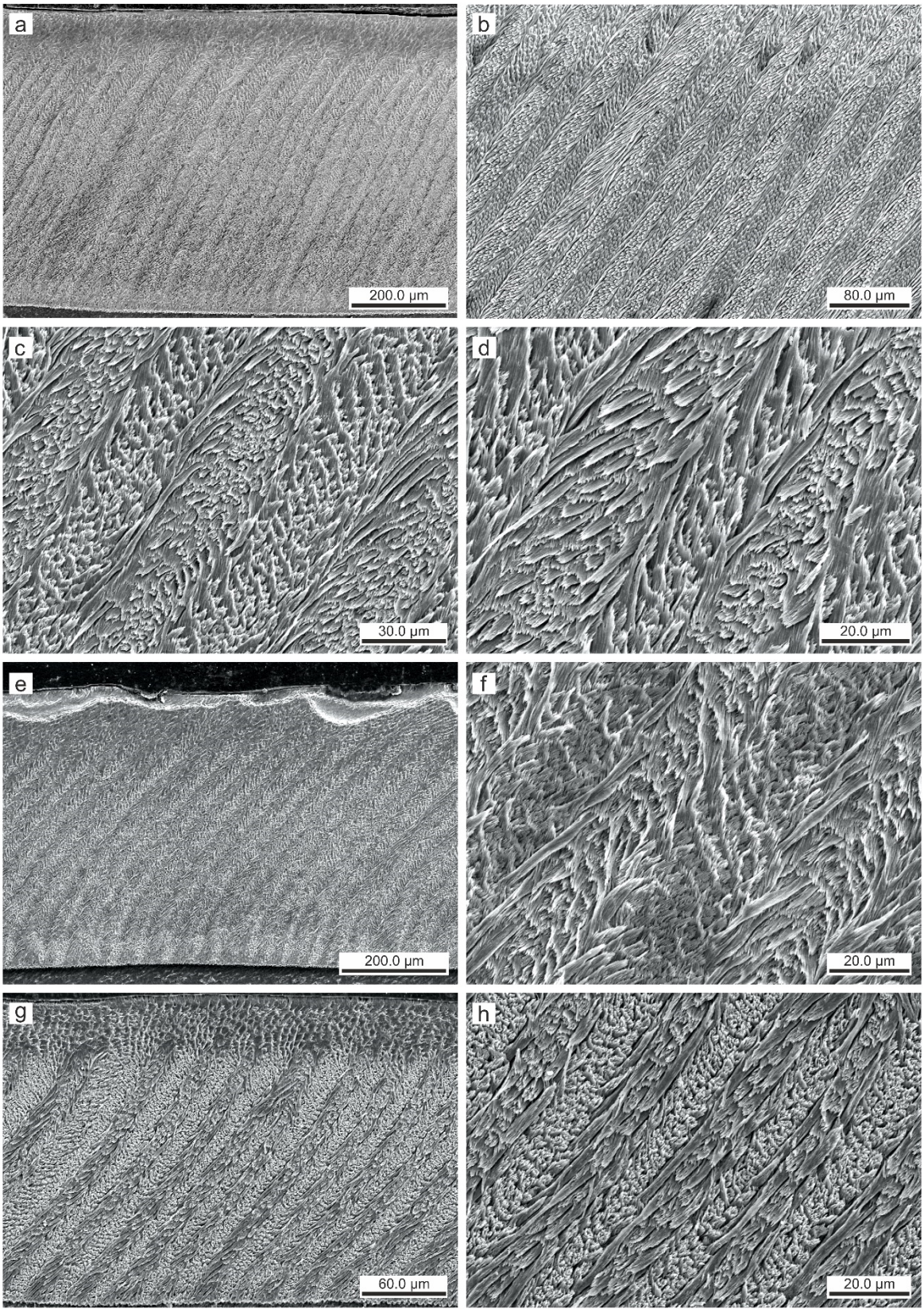

Fig. 8 Scanning electron photomicrographs of incisors of the subfossil giant hutias *Amblyrhiza* from St. Barth, and of the chinchilloid *Borikenomys* from the lower Oligocene of Puerto Rico, for which the enamel microstructure (multiserial HSBs) is shown in longitudinal section and at different magnifications (overview of the enamel layer and details of the microstructure in PI). **a–d** *Amblyrhiza* sp. (UM SB-Coco-03); **e–f** *Amblyrhiza* sp. (juvenile; UM SB-Coco-04); **g–h** *Borikenomys praecursor* (LACM 162956)

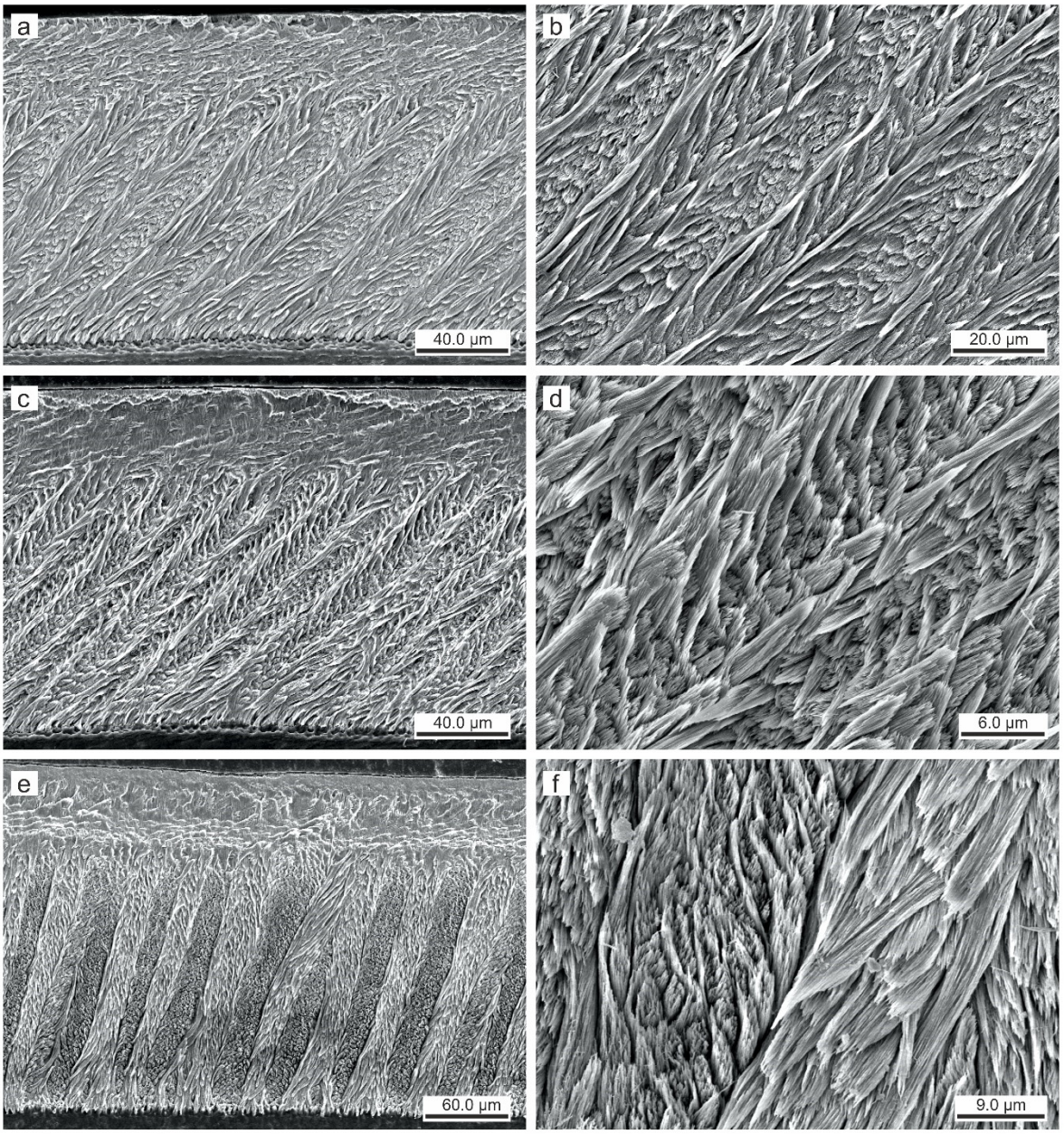

Fig. 9 Scanning electron photomicrographs of incisors of extant caviomorph rodents (Chinchillidae Chinchilloidea and Cuniculidae Cavioidea) from South America, for which the enamel microstructure (multiserial HSBs) is shown in longitudinal section and at different magnifications. The left pictures illustrate an overview of the enamel layer for each specimen, and the associated right ones a detail of the microstructure in PI. **a–b** *Lagidium* sp. (UM 521N, reversed); **c–d** *Chinchilla* sp. (UM N312, reversed); **e–f** *Cuniculus paca* (UM N385)

Taxa	Specimen number	Designation (locus)	Provenance	Age	Miscellaneous (collector, collection, date)
Isolobodon portoricensis	UF 520141 (FMNH)	Right lower incisor (frag.) [partial mandible]	Cueva de las Abejas (XD007), Pedernales, Dominican Republic	Late Pleistocene or Holocene (Santarosean)	C. A. Woods (02/1984)
Isolobodon montanus	UF 333712 (FMNH)	Left lower incisor (frag.) [mandible i1 p4–m3]	Trouing Jeremie 5 (XH007), Dept. du Sud, Haiti	Holocene	(07/07/1985)
Hexolobodon phenax	UF 520143 (FMNH)	Right lower incisor [partial mandible]	Trouing Marassa/Trujin Bridge (XH002), Dpt. de l'Ouest, Haiti	Holocene	(10, 35, 21. B; 31/07/1983)
Rhizoplagiodontia lemkei	UF 70850 (FMNH)	Right lower incisor [mandible i1 m1–m2]	Trouing Jeremie 5 (XH007), Dept. du Sud, Haiti	Late Pleistocene or Holocene	C. A. Woods (01/02/1980)
Plagiodontia ipnaeum [velozi]	UF 520142 (FMNH)	Left upper incisor	Trouing Bois Formon 3 (XH019), Dept. du Sud, Haiti	Late Pleistocene or Holocene (Santarosean)	D. Codier (25/01/1984)
Capromys pilorides lewisi	UF 520144 (FMNH)	Left upper incisor	Dolphin Cave (XC018), Grand Cayman Co., Cayman Islands	Late Pleistocene or Holocene	G. S. Morgan (31/03/1993)
Geocapromys caymanensis	UF 520145 (FMNH)	Right lower incisor	Dolphin Cave (XC018), Grand Cayman Co., Cayman Islands	Late Pleistocene or Holocene	G. S. Morgan (31/03/1993)
Geocapromys columbianus	CLV 2595	Right lower incisor	Cueva del Infierno, Mayabeque, Cuba	Middle–late Holocene (Archaeological site)	Coll. S. Diaz Franco
Macrocapromys acevedo	CLV 401	Right lower incisor (frag.)	Cantera J4 # 1, Matanzas, Cuba	Late Pleistocene–Holocene	Coll. L. W. Viñola López (16/05/2012)
Mesocapromys nanus	CLV 2597	Left lower incisor	Cantera J4 # 1, Matanzas, Cuba	Late Pleistocene–Holocene	Coll. L. W. Viñola López (2011)
Mysateles sp.	UM 524N	Left lower incisor [mandible i1 p4–m3]	Cuba (area of capture not specified)	Recent	Old UM collection
Brotomys contractus	UF 333716	Left upper incisor [pmx + mx; I1 P3]	Trou Jean Paul (XH013H) (suf. Layer), Dept. de l'Ouest, Haiti	Not specified	(16/02/1984)
Boromys offella	CLV 2596	Left lower incisor (frag.)	Cueva del Infierno, Mayabeque, Cuba	Middle–late Holocene (Archaeological site)	Coll. S. Diaz Franco
Boromys torrei	CLV 2598	Right upper incisor	Cuevas Blancas, Mayabeque, Cuba	Holocene (see Orihuela et al. 2020)	Coll. E. Fonseca and O. Jimenez (01/05/2001)
Heteropsomys sp.	UPRMP-3229	Left lower incisor	*Elasmodontomys* Shelter, Manatí, Puerto Rico	Late Pleistocene (~ 60 ka; Tarentian)	J. Vélez-Juarbe, L. Marivaux et al. (05-06/02/2020)
Elasmodontomys obliquus	UPRMP-3230	Right lower incisor	*Elasmodontomys* Shelter, Manatí, Puerto Rico	Late Pleistocene (~ 60 ka; Tarentian)	J. Vélez-Juarbe, L. Marivaux et al. (05-06/02/2020)
Elasmodontomys obliquus	UPRMP-3231	Left lower incisor	*Elasmodontomys* Shelter, Manatí, Puerto Rico	Late Pleistocene (~ 60 ka; Tarentian)	J. Vélez-Juarbe, L. Marivaux et al. (05-06/02/2020)
Elasmodontomys obliquus	UPRMP-3232	Right lower incisor	*Elasmodontomys* Shelter, Manatí, Puerto Rico	Late Pleistocene (~ 60 ka; Tarentian)	J. Vélez-Juarbe, L. Marivaux et al. (05-06/02/2020)
Clidomys sp. (*osborni*?)	UF 274295	Lower or upper incisor (frag.)	Wallingford 1 (XJ002), St. Elizabeth Parish, Jamaica	Pleistocene	T. H. Patton (06/1966)
Amblyrhiza sp. (*inundata*?)	UM SB-Coco-03	Lower incisor	Fissure-filling 01, Îlet Coco, satellite islet of St. Barthélemy	Middle Pleistocene (~ 415 ka; Chibanian)	L. Marivaux, G. Maincent and P. Münch (25/05/2019)
Amblyrhiza sp. (juvenile)	UM SB-Coco-04	Left small lower incisor (frag.)	Fissure-filling 01, Îlet Coco, satellite islet of St. Barthélemy	Middle Pleistocene (~ 415 ka; Chibanian)	L. Marivaux, G. Maincent and P. Münch (25/05/2019)
Borikenomys praecursor	LACM 162956	Lower incisor (frag.)	LACM Loc. 8060, Río Guatemala, San Sebastián, Puerto Rico	Late early Oligocene (~29.5 Ma)	J. Vélez-Juarbe, L. Marivaux et al. (10/02/2020)
Lagidium sp.	UM 521N	Left lower incisor [mandible i1 p4–m3]	South America (provenance not specified)	Recent (1946)	Old UM collection
Chinchilla sp.	UM N312	Left lower incisor [mandible i1 p4–m3]	South America (provenance not specified)	Recent	Old UM collection
Cuniculus paca	UM N385	Right lower incisor [mandible i1 p4–m3]	South America (provenance not specified)	Recent	Old UM collection

Taxon		Specimen number	Incisor type	Incisor labial surface	Incisor width (mm)	Enamel thickness (µm)	% of PE	Inclination of HSBs	Prisms per HSB	Prisms of transitional zone	Division HSB	Prism cross section in PI	IPM configuration in PI	IPM anastomosis	Angle (α) crystallites of IPM/prisms	Subtype	Figure
Isolobodon portoricensis	†	UF 520141	Lower	Flat, smooth	2.29	411	11	40°	3–4	Not well-marked (1)	Absent	Oval to flattened	Inter-row thin sheets	None	# Rectangular (83–90°)	3	3a–b
Isolobodon montanus	†	UF 333712	Lower	Flat, smooth	2.96	307	6	29–32°	4–5	Absent	Absent	Oval to flattened	Inter-row thin sheets	None	# Rectangular (80–84°)	3	3c–d
Hexolobodon phenax	†	UF 520143	Lower	Flat, smooth	3.18	531	8	23–28°	4	Absent	Absent	Flattened	Inter-row thin sheets	Possible but rare	# Rectangular (81–87°)	3	3e–f
Rhizoplagiodontia lemkei	†	UF 70850	Lower	Slightly convex, smooth	2.37	400	< 5	40–44°	3(–4)	Not well-marked (1)	Absent	Oval to flattened	Inter-row thin sheets	None	# Rectangular (85–87°)	3	3g–h
Plagiodontia ipnaeum	†	UF 520142	Upper	Flat, smooth	5.04	388	7	38°	4(–5)	Not well-marked (1)	Absent	Oval	Inter-row thin sheets	None	# Rectangular (84–88°)	3	4a–b
Capromys pilorides lewisi	†	UF 520144	Upper	Flat, smooth	3.26	508	8	26–27°	5–6	Absent	Absent	Oval to flattened	Inter-row thin sheets	None	Rectangular (89–90°)	3	4c–d
Geocapromys caymanensis	†	UF 520145	Lower	Flat, smooth	2.07	259	6	36–38°	5	Absent	Very rare	Oval to flattened	Inter-row thin sheets	None	# Rectangular (82–84°)	3	4e–f
Geocapromys columbianus	†	CVL 2595	Lower	Flat, smooth	2.07	254	3	39°	4–5	Absent	Absent	Oval	Inter-row thin sheets	Possible but very rare	# Rectangular (83–87°)	3	4g–h
Macrocapromys acevedo	†	CLV 401	Lower	Slightly convex, smooth	3.70	232	7	23°	3(–4)	Not well-marked (1)	Absent	Flattened	Inter-row thin sheets	None	Rectangular (88–90°)	3	5a–b
Mesocapromys nanus	†	CLV 2597	Lower	Flat, smooth	1.33	208	14	48–50°	3	Present (1)	Absent	Flattened	Inter-row thin sheets	None	Sub–rectangular (75–80°)	3	5c–d
Mysateles sp.		UM 524N	Lower	Flat, smooth	2.44	298	16	35°	3(–4)	Not well-marked (1)	Very rare	Flattened	Inter-row thin sheets	None	Rectangular (87–88°)	3	5e–f
Brotomys contractus	†	UF 333716	Upper	Flat, smooth	1.55	279	12	18–22°	3(–4)	Present (1–2)	Absent	Rounded to oval	Inter-row thin sheets	None	Rectangular (~89°)	3	6a–b
Boromys offella	†	CLV 2596	Lower	Flat, smooth	1.51	298	10	32–33°	3(–4)	Not well-marked (1)	Very rare	Oval to flattened	Inter-row thin sheets	Possible but very rare	Rectangular (85–90°)	3	6c–d
Boromys torrei	†	CLV 2598	Upper	Flat, smooth	0.92	256	12	20–25°	3(–4)	Present (1)	Rare	Oval to flattened	Inter-row thin sheets	None	Rectangular (90°)	3	6e–f
Heteropsomys sp.	†	UPRMP-3229	Lower	Flat, smooth	3.04	256	10	35–36°	4(–5)	Present (1)	Absent	Oval	Inter-row thin sheets	Possible but very rare	Sub–rectangular (75–79°)	3	6g–h
Elasmodontomys obliquus	†	UPRMP-3230	Lower	Flat, two shallow sulci	4.88	275	10	27–30°	4–5	Present (1)	Absent	Oval to flattened	Inter-row and often inter-prism thin sheets	Very frequent and regular	Low acute (20–24°)	(1–)2	7a–b
Elasmodontomys obliquus	†	UPRMP-3231	Lower	Flat, two shallow sulci	4.59	232	15	35–37°	4–5	Present (1–2)	Absent	Oval to flattened	Inter-row and often inter-prism thin sheets	Very frequent and regular	Low acute (16–24°)	(1–)2	7c–d
Elasmodontomys obliquus	†	UPRMP-3232	Lower	Flat, two well-defined sulci	5.33	232	17	28–31°	4(–5)	Present (1–2)	Very rare	Rounded to flattened	Inter-row and often inter-prism thin sheets	Very frequent and regular	Low acute (23–26°)	(1–)2	7e–f
Clidomys sp.	†	UF 274295	Lower or upper	Strongly convex, smooth	5.48	254	10	12–15°	(3–)5	Not well-marked (1)	Very rare	Flattened	Inter-row and inter-prism thin sheets (sheath-like)	Permanent	Parallel (~10° or less)	1	7g–h
Amblyrhiza sp.	†	UM SB-Coco-03	Lower	Flat, crenulated (multi-sulci)	11.26	(660–)752	10–13	25–34°	5(–6)	Present (1–2)	Absent	Oval to flattened	Inter-row and often inter-prism thin sheets	Very frequent and regular	Low acute (28–35°)	2	8a–d
Amblyrhiza sp. (juvenile)	†	UM SB-Coco-04	Lower	Flat, crenulated (multi-sulci)	6.59	528	9	42° (main axis)	4(–6)	Present (1)	Absent	Oval to flattened	Inter-row and often inter-prism thin sheets	Very frequent and regular	Low acute (28–36°)	2	8e–f
Borikenomys praecursor	†	LACM 162956	Lower	Flat, smooth	2.59	218	18	37–41°	3(–4)	Not well-marked (1)	Very rare	Rounded to oval	Inter-row and often inter-prism thin sheets	Very frequent and regular	Low acute (29–35°)	2	8g–h
Lagidium sp.		UM 521N	Lower	Flat, smooth	1.74	144	19	45°	3(–4)	Present (1–2)	Very rare	Oval to flattened	Inter-row and inter-prism thin sheets (sheath-like)	Permanent	# Parallel (~15–22°)	1(–2)	9a–b
Chinchilla sp.		UM N312	Lower	Flat, smooth	1.70	149	21	46–49°	3(–4)	Present (1–2)	Very rare	Flattened	Inter-row and often inter-prism thin sheets	Very frequent and regular	Low acute (22–28°)	(1–)2	9c–d
Cuniculus paca		UM N385	Lower	Strongly convex, smooth	3.70	248	22	17°	4	Absent	Frequent	Flattened	Inter-row and inter-prism thin sheets (sheath-like)	Permanent	# Parallel (~15° or less)	1	9e–f

PARVORDER and Superfamily	Family	Subfamily	Species / Specimen number	Taxonomic remark*	Age	Locality (Loc.) and/or Formation (Fm.) for extinct species	Multiserial subtype (sbt)	References regarding the enamel microstructure
New World HYSTRICOGNATHI								
CAVIOMORPHA								
Erethizontoidea	Erethizontidae	Erethizontinae	*Steiromys* sp.		Late early Miocene	Arroyo Elke, Santa Cruz Fm., Argentina	Multiserial sbt 1	Martin (1992)
			Steiromys sp.				Multiserial sbt 1–2	Martin (1994b)
			Eosteiromys segregatus	*Steiromys segregatus* sensu Martin	Early Miocene	Southern Cliff of Lake Colhué Huapi (Gran Barranca; Sarmiento Fm.), Argentina	Multiserial sbt 2	Martin (1992, 1994b)
			Coendu mexicanus		Recent		Multiserial sbt 1	Martin (1992, 1994b)
			Coendou prehensilis	*Coendu prehensilis* sensu Martin	Recent		Multiserial sbt 1–2 & 2	Martin (1994b)
			Coendou quichua	*Coendu rothschildi* sensu Martin	Recent		Multiserial sbt 2	Martin (1994b)
			Erethizon dorsatum		Recent		Multiserial sbt 2	Martin (1992)
			Erethizon dorsatum		Recent		Multiserial sbt 1–2	Martin (1994b)
		Chaetomyinae	*Chaetomys subspinosus*		Recent		Multiserial sbt 1–2	Martin (1992)
Cavioidea	Dasyproctidae		*Dasyprocta fuliginosa*		Recent		Multiserial sbt 2	Martin (1992)
			Myoprocta acouchy		Recent		Multiserial sbt 2	Martin (1992)
	Cuniculidae		*Cuniculus paca*	*Agouti paca* sensu Martin	Recent		Multiserial sbt 1	Martin (1992)
	Caviidae		*Eocardia* sp.		Early Miocene	10 miles south of Coy Inlet (?Santa Cruz Fm.), Argentina	Multiserial sbt 2	Martin (1992)
			Eocardia perforata		Late early Miocene	Santa Cruz Fm., Argentina	Multiserial sbt 2	Martin (1992)
			Neoreomys australis		Late early Miocene	Santa Cruz Fm., Argentina	Multiserial sbt 1	Martin (1992)
		Caviinae	*Branisamys luribayensis*		Late early Oligocene – late Oligocene	Salla (Salla Beds), Bolivia	Multiserial sbt 2	Martin (1992)
			Cavia porcellus		Recent		Multiserial sbt 1	Martin (1992)
			Galea sp.		Recent		Multiserial sbt 1	Martin (1992)
		Dolichotinae	cf. *Prodolichotis* sp.		Miocene	V 4936 (Honda Fm.), Colombia	Multiserial sbt 2	Martin (1992)
			Dolichotis patagonum		Recent		Multiserial sbt 2	Martin (1992)
		Hydrochoerinae	*Cardiomys ameghinorum*		Pliocene	Corral Quemado (Corral Quemado Fm.), Argentina	Multiserial sbt 2	Martin (1992)
			Cardiatherium sp.		?	Delta-Bereich (unnamed Fm.), Argentina	Multiserial sbt 1	Martin (1992)
			Neochoerus sp.		Pliocene	Graham Co. (It. Blanca), Arizona	Multiserial sbt 1	Martin (1992)
			Hydrochoerus hydrochaeris	*Hydrochaeris hydrochaeris* sensu Martin	Recent		Multiserial sbt 1	Martin (1992)
Chinchilloidea			*Incamys* sp.		Late early Oligocene – late Oligocene	VI, Torrolo, Salla?, Bolivia	Multiserial sbt 2	Martin (1992, 1994a)
			Incamys bolivianus		Late early Oligocene – late Oligocene	Salla (Salla Beds), Bolivia	Multiserial sbt 2	Martin (1993)
	Dinomyidae		*"Scleromys" colombianus*		Late middle Miocene	V 4517 and V 4519, La Venta (Honda Group), Colombia	Multiserial sbt 2	Martin (1992, 1994a)
			Drytomomys aequatorialis	*"Olenopsis" aequatorialis* sensu Martin	Late middle Miocene	UC Loc. V 4518 and Lone Tree Loc. V 4521 , La Venta (Honda Group), Colombia	Multiserial sbt 2	Martin (1992)
			Eumegamys ameghinorum		?	Delta-Bereich (unnamed Fm.), Argentina	Multiserial sbt 2	Martin (1992)
			Tetrastylus cf. *diffusus*		Early Pliocene	Santa Maria Valley (Chiquimil B Fm.), Argentina	Multiserial sbt 2	Martin (1992)
			Dinomys branickii		Recent		Multiserial sbt 2	Martin (1992)
	Chinchillidae		*Scotamys antiquus*		Late early Oligocene – late Oligocene	Cabeza Blanca and La Flecha (Sarmiento Fm.), Argentina	Multiserial sbt 2	Martin (1992)
		Chinchillinae	*Chinchilla lanigera*		Recent		Multiserial sbt 1	Martin (1992)
			Lagidium sp.	*Lagidium peruanum* sensu Martin	Recent		Multiserial sbt 1	Martin (1992)
			Lagidium viscacia		Recent		Multiserial sbt 2	Martin (1992)
		Lagostominae	*Perimys procerus*		Late early Miocene	Santa Cruz Fm., Argentina	Multiserial sbt 1	Martin (1992)
			Lagostomus sp.	*Lagostomopsis* sp. sensu Martin	Pliocene	Corral Quemado (Corral Quemado Fm.) and V 76057 (Chapadamalal Fm.), Argentina	Multiserial sbt 2	Martin (1992)
Octodontoidea			*Platypittamys brachyodon*		Late early Oligocene – late Oligocene	Scaritt Pocket (Sarmiento Fm.), Argentina	Multiserial sbt 3	Martin (1992, 1994a)
			Sallamys sp.		Late early Oligocene – late Oligocene	Salla (Salla Beds), Bolivia	Multiserial sbt 2	Martin (1992)
			Sallamys pascuali		Late early Oligocene – late Oligocene	Salla (Salla Beds), Bolivia	Multiserial sbt 2	Martin (1992)
			Sallamys		Late early Oligocene – late Oligocene	Salla (Salla Beds), Bolivia	Multiserial sbt 2–3	Martin (1994a)
			Acarechimys sp.		Late early Miocene	Argentina	Multiserial sbt 3	Martin (1992, 1994b)
			Caviocricetus lucasi		Early Miocene	Bryn Gwyn and Gran Barranca (Sarmiento Fm.), Paso Córdoba (Chinchinales Fm.) and Cerro Bandera (Cerro Bandera Fm.), Argentina	Multiserial sbt 2–3	Vieytes (2003), Vucetich et al. (2010, 2015), Arnal et al. (2014)
			Protadelphomys		Early Miocene	Gran Brranca, Bryn Gwyn, Sacanana (Sarmiento Fm.), Argentina	Multiserial sbt 2–3	Vieytes (2003), Vucetich et al. (2010, 2015)
			Willidewu		Early Miocene	Paso Córdoba (Chinchinales Fm.) and Bryn Gwyn (Sarmiento Fm.), Argentina	Multiserial sbt 2–3	Vieytes (2003), Vucetich et al. (2015)
			Dudumus ruigomezi		Early Miocene	Bryn Gwyn (Sarmiento Fm.), Argentina	Multiserial sbt 3	Arnal et al. (2014)
			Sciamys principalis		Late early Miocene	in the vivinity of Canon de los Vucas (25 miles south of Mt. Leon; Santa Cruz Fm.), Argentina	Multiserial sbt 3	Martin (1992)
			Spaniomys riparius		Late early Miocene	Santa Cruz Fm., Argentina	Multiserial sbt 3	Martin (1992)
			Protacaremys prior	*Protacaremys prius* sensu Martin	Early Miocene	Colhué Huapi (Gran Barranca; Sarmiento Fm.), Argentina	Multiserial sbt 3	Martin (1992)
			Plesiacarechimys koenigswaldi		Middle Miocene	Estancia Cerro San Antonio (Collon Cura Fm.), Argentina	Multiserial sbt 2–3	Vucetich and Vieytes (2006)
			Adelphomys sp.		Late early Miocene	Argentina	Multiserial sbt 3	Martin (1992, 1994a)
			Stichomys regularis		Late early Miocene	Coy Inlet (Santa Cruz Fm)., Argentina	Multiserial sbt 3	Martin (1992, 1994a)
	Abrocomidae		*Abrocoma bennetti*		Recent		Multiserial sbt 3	Martin (1992)
	Octodontidae		*Aconaemys fuscus*		Recent		Multiserial sbt 3	Martin (1992)
			Octodon degus		Recent		Multiserial sbt 3	Martin (1992)
			Octodon 'bridgesi'		Recent		Multiserial sbt 3	Vieytes et al. (2007)
			Octodontomys gliroides		Recent		Multiserial sbt 3	Martin (1992)
			Spalacopus cyanus		Recent		Multiserial sbt 3	Martin (1992)
	Ctenomyidae		*Ctenomys* sp.		Sub-Recent		Multiserial sbt 3	Martin (1992)
			Ctenomys maulinus		Recent		Multiserial sbt 3	Martin (1992)
			Ctenomys sp. 'perucho'		Recent		Multiserial sbt 3	Morgan et al. (2017)
			Ctenomys australis		Recent		Multiserial sbt 3	Vieytes et al. (2007), Morgan et al. (2017)
			Ctenomys talarum		Recent		Multiserial sbt 3	Vieytes et al. (2007), Morgan et al. (2017)
			Ctenomys chapalmalensis		Late Pliocene	Punta San Andrés (San Andrés Fm.), Argentina	Multiserial sbt 3	Vieytes et al. (2007)
	Echimyidae	Echimyinae	*Dactylomys dactylinus*		Recent		Multiserial sbt 3	Martin (1992, 1994b)

PARVORDER and Superfamily	Family	Subfamily	Species / Specimen number	Taxonomic remark*	Age	Locality (Loc.) and/or Formation (Fm.) for extinct species	Multiserial subtype (sbt)	References regarding the enamel microstructure
			Dactylomys boliviensis		Recent		Multiserial sbt 3	Vieytes et al. (2007)
			Kannabateomys amblyonyx		Recent		Multiserial sbt 3	Martin (1992, 1994a, b)
			Echimyinae indet.	*Loncheres* sp. sensu Martin	Recent		Multiserial sbt 3	Martin (1992)
			Diplomys labilis		Recent		Multiserial sbt 3	Martin (1992)
			Toromys/Makalata grandis	*Echimys grandis* sensu Martin	Recent		Multiserial sbt 3	Martin (1992, 1994b)
			Makalata armata		Recent		Multiserial sbt 3	Martin (1992, 1994b)
			Isothrix villosus		Recent		Multiserial sbt 3	Martin (1992, 1994b)
			Hoplomys gymnurus		Recent		Multiserial sbt 3	Martin (1992)
			Mesomys stimulax		Recent		Multiserial sbt 3	Martin (1992)
			Proechimys roberti	*Proechimys oris* sensu Martin	Recent		Multiserial sbt 3	Martin (1992)
			Trichomys apereoides	*Nelomys antricola* sensu Martin	Recent		Multiserial sbt 3	Martin (1992)
			Myocastor coypus		Recent		Multiserial sbt 3	Martin (1992)
		Euryzygomatomyinae	*Clyomys laticeps*		Recent		Multiserial sbt 3	Martin (1992)
		Carterodontinae	*Carterodon sulcidens*		Recent		Multiserial sbt 3	Martin (1992, 1994b)
		Capromyinae	*Capromys pilorides*		Recent		Multiserial sbt 3	Martin (1992)
		(Isolobodontinae)	*Isolobodon portoricensis*	*Isolobodon levir* sensu Martin	Pleistocene–Holocene	Ft. Liberté, Haiti, Antilles	Multiserial sbt 3	Martin (1992)
		Heteropsomyinae	*Boromys torrei*		Pleistocene–Holocene	Caves at Daiquiri, Cuba, Antilles	Multiserial sbt 3	Martin (1992)
			Brotomys voratus		Pleistocene–Holocene	Ft. Liberté, Haiti, Antilles	Multiserial sbt 3	Martin (1992, 1994b)
Incertae sedis **extinct superfamily**								
	Cephalomyidae		*Cephalomys arcidens*		Late early Oligocene – late Oligocene	Rio Chico del Chubut, Argentina	Multiserial sbt 1	Martin (1992)
			Cephalomys bolivianus		Late early Oligocene – late Oligocene	Salla-Luribay (Salla Beds), Bolivia	Multiserial sbt 2	Martin (1993)
	"Heptaxodontidae"		*Amblyrhiza* sp.		Pleistocene	Devil's Hole (for AMNH 125642), St. Martin, Antilles	Multiserial sbt 2	Martin (1992)
			Elasmodontomys obliquus		Pleistocene	Cueva Clara, Puerto Rico, Antilles	Multiserial sbt 2	Martin (1992)
			LACM 145444		Early Oligocene	Santa Rosa (upper Yahuarango Fm. or Pozo Fm. or lower Chambira Fm.), Peru	Multiserial sbt 1	Martin (2004)
			LACM 149417		Early Oligocene	Santa Rosa (upper Yahuarango Fm. or Pozo Fm. or lower Chambira Fm.), Peru	Multiserial sbt 1	Martin (2005)
			LACM 149421		Early Oligocene	Santa Rosa (upper Yahuarango Fm. or Pozo Fm. or lower Chambira Fm.), Peru	Multiserial sbt 1	Martin (2005)
			LACM 149423		Early Oligocene	Santa Rosa (upper Yahuarango Fm. or Pozo Fm. or lower Chambira Fm.), Peru	Multiserial sbt 1	Martin (2005)
			LACM 149424		Early Oligocene	Santa Rosa (upper Yahuarango Fm. or Pozo Fm. or lower Chambira Fm.), Peru	Multiserial sbt 1	Martin (2005)
			LACM 145447		Early Oligocene	Santa Rosa (upper Yahuarango Fm. or Pozo Fm. or lower Chambira Fm.), Peru	Multiserial sbt 1–2	Martin (2004)
			LACM 145446		Early Oligocene	Santa Rosa (upper Yahuarango Fm. or Pozo Fm. or lower Chambira Fm.), Peru	Multiserial sbt 1–2	Martin (2004)
			LACM 149405		Early Oligocene	Santa Rosa (upper Yahuarango Fm. or Pozo Fm. or lower Chambira Fm.), Peru	Multiserial sbt 1–2	Martin (2005)
			LACM 149407		Early Oligocene	Santa Rosa (upper Yahuarango Fm. or Pozo Fm. or lower Chambira Fm.), Peru	Multiserial sbt 1–2	Martin (2005)
			LACM 149408		Early Oligocene	Santa Rosa (upper Yahuarango Fm. or Pozo Fm. or lower Chambira Fm.), Peru	Multiserial sbt 1–2	Martin (2005)
			LACM 149410		Early Oligocene	Santa Rosa (upper Yahuarango Fm. or Pozo Fm. or lower Chambira Fm.), Peru	Multiserial sbt 1–2	Martin (2005)
			LACM 149412		Early Oligocene	Santa Rosa (upper Yahuarango Fm. or Pozo Fm. or lower Chambira Fm.), Peru	Multiserial sbt 1–2	Martin (2005)
			LACM 149413		Early Oligocene	Santa Rosa (upper Yahuarango Fm. or Pozo Fm. or lower Chambira Fm.), Peru	Multiserial sbt 1–2	Martin (2005)
			LACM 149416		Early Oligocene	Santa Rosa (upper Yahuarango Fm. or Pozo Fm. or lower Chambira Fm.), Peru	Multiserial sbt 1–2	Martin (2005)
			LACM 149418		Early Oligocene	Santa Rosa (upper Yahuarango Fm. or Pozo Fm. or lower Chambira Fm.), Peru	Multiserial sbt 1–2	Martin (2005)
			LACM 149419		Early Oligocene	Santa Rosa (upper Yahuarango Fm. or Pozo Fm. or lower Chambira Fm.), Peru	Multiserial sbt 1–2	Martin (2005)
			LACM 149420		Early Oligocene	Santa Rosa (upper Yahuarango Fm. or Pozo Fm. or lower Chambira Fm.), Peru	Multiserial sbt 1–2	Martin (2005)
			LACM 149422		Early Oligocene	Santa Rosa (upper Yahuarango Fm. or Pozo Fm. or lower Chambira Fm.), Peru	Multiserial sbt 1–2	Martin (2005)
			LACM 145445		Early Oligocene	Santa Rosa (upper Yahuarango Fm. or Pozo Fm. or lower Chambira Fm.), Peru	Multiserial sbt 2	Martin (2004)
			LACM 149406		Early Oligocene	Santa Rosa (upper Yahuarango Fm. or Pozo Fm. or lower Chambira Fm.), Peru	Multiserial sbt 2	Martin (2005)
			LACM 149411		Early Oligocene	Santa Rosa (upper Yahuarango Fm. or Pozo Fm. or lower Chambira Fm.), Peru	Multiserial sbt 2	Martin (2005)
			LACM 149415		Early Oligocene	Santa Rosa (upper Yahuarango Fm. or Pozo Fm. or lower Chambira Fm.), Peru	Multiserial sbt 2	Martin (2005)
			LACM 145442		Early Oligocene	Santa Rosa (upper Yahuarango Fm. or Pozo Fm. or lower Chambira Fm.), Peru	Multiserial sbt 3	Martin (2004)
			LACM 145443		Early Oligocene	Santa Rosa (upper Yahuarango Fm. or Pozo Fm. or lower Chambira Fm.), Peru	Multiserial sbt 3	Martin (2004)
			LACM 149409		Early Oligocene	Santa Rosa (upper Yahuarango Fm. or Pozo Fm. or lower Chambira Fm.), Peru	Multiserial sbt 3	Martin (2005)
			LACM 149414		Early Oligocene	Santa Rosa (upper Yahuarango Fm. or Pozo Fm. or lower Chambira Fm.), Peru	Multiserial sbt 3	Martin (2005)
			MPEF 7962		Late early Oligocene	La Cantera (Sarmiento Fm.), Argentina	Multiserial sbt 1 or 1–2	Vucetich et al. (2010)
			MPEF 7963		Late early Oligocene	La Cantera (Sarmiento Fm.), Argentina	Multiserial sbt 2–3	Vucetich et al. (2010)
			MPEF 7964		Late early Oligocene	La Cantera (Sarmiento Fm.), Argentina	Multiserial sbt 2	Vucetich et al. (2010)
			MPEF 7965		Late early Oligocene	La Cantera (Sarmiento Fm.), Argentina	Multiserial sbt 2–3	Vucetich et al. (2010)
(Chinchilloidea)	(?Dinomyidae)	Caviomorpha gen. et sp. indet. A	MA 316	(*Borikenomys paecursor*)	Late early Oligocene (Rupelian)	West bank of Río Guatemala (San Sebastian Fm.), Puerto Rico	Multiserial sbt 2	Martin in Vélez-Juarbe et al. (2014), Marivaux et al. (2020)
		Caviomorpha gen. et sp. indet. B	MA 308		Late Oligocene (Chattian)	West-facing roadcut along road PR-111 (Mudstone unit within the Lares Limestone), Puerto Rico	Multiserial sbt 2	Martin in Vélez-Juarbe et al. (2014)
			MUSM 2649		Late middle Eocene -> late Eocene	Contamana CTA-47 (lower mb. Pozo Fm.), Peru	Multiserial sbt 2	Boivin et al. (2019a)
			MUSM 2650		Late middle Eocene -> late Eocene	Contamana CTA-47 (lower mb. Pozo Fm.), Peru	Multiserial sbt (1)-2	Boivin et al. (2019a)
			MUSM 2803		Late middle Eocene -> late Eocene	Contamana CTA-27 (lower mb. Pozo Fm.), Peru	Multiserial sbt 1	Boivin et al. (2019a)
			MUSM 2804		Late middle Eocene -> late Eocene	Contamana CTA-27 (lower mb. Pozo Fm.), Peru	Multiserial sbt 2	Boivin et al. (2019a)
			MUSM 2805		Late middle Eocene -> late Eocene	Contamana CTA-27 (lower mb. Pozo Fm.), Peru	Multiserial sbt 2	Boivin et al. (2019a)
			MUSM 2806		Late middle Eocene -> late Eocene	Contamana CTA-27 (lower mb. Pozo Fm.), Peru	Multiserial sbt 2	Boivin et al. (2019a)
			MUSM 2807		Late middle Eocene -> late Eocene	Contamana CTA-27 (lower mb. Pozo Fm.), Peru	Multiserial sbt 2	Boivin et al. (2019a)
			MUSM 2808		Late middle Eocene -> late Eocene	Contamana CTA-27 (lower mb. Pozo Fm.), Peru	Multiserial sbt 2	Boivin et al. (2019a)
			MUSM 2809		Late middle Eocene -> late Eocene	Contamana CTA-27 (lower mb. Pozo Fm.), Peru	Multiserial sbt 2	Boivin et al. (2019a)
			MUSM 2810		Late middle Eocene -> late Eocene	Contamana CTA-27 (lower mb. Pozo Fm.), Peru	Multiserial sbt 2	Boivin et al. (2019a)
			MUSM 2811		Late middle Eocene -> late Eocene	Contamana CTA-27 (lower mb. Pozo Fm.), Peru	Multiserial sbt 2	Boivin et al. (2019a)
			MUSM 2812		Late middle Eocene -> late Eocene	Contamana CTA-27 (lower mb. Pozo Fm.), Peru	Multiserial sbt 2	Boivin et al. (2019a)

PARVORDER and Superfamily	Family	Subfamily	Species / Specimen number	Taxonomic remark*	Age	Locality (Loc.) and/or Formation (Fm.) for extinct species	Multiserial subtype (sbt)	References regarding the enamel microstructure
			MUSM 2813		Late middle Eocene -> late Eocene	Contamana CTA-27 (lower mb. Pozo Fm.), Peru	Multiserial sbt 2	Boivin et al. (2019a)
			MUSM 2814		Late middle Eocene -> late Eocene	Contamana CTA-27 (lower mb. Pozo Fm.), Peru	Multiserial sbt 2	Boivin et al. (2019a)
			MUSM 2815		Late middle Eocene -> late Eocene	Contamana CTA-27 (lower mb. Pozo Fm.), Peru	Multiserial sbt 2	Boivin et al. (2019a)
			MUSM 2816		Late middle Eocene -> late Eocene	Contamana CTA-27 (lower mb. Pozo Fm.), Peru	Multiserial sbt 2	Boivin et al. (2019a)
			MUSM 2817		Late middle Eocene -> late Eocene	Contamana CTA-27 (lower mb. Pozo Fm.), Peru	Multiserial sbt 1-(2)	Boivin et al. (2019a)
			MUSM 2840		Late middle Eocene -> late Eocene	Contamana CTA-29 (lower mb. Pozo Fm.), Peru	Multiserial sbt 2	Boivin et al. (2019a)
			MUSM 2873		Late Oligocene	Contamana CTA-32 (Chambira Fm.), Peru	Multiserial sbt 2	Boivin et al. (2019a)
			MUSM 2902		Late Oligocene	Contamana CTA-61 (Chambira Fm.), Peru	Multiserial sbt 1-(2)	Boivin et al. (2019a)
			MUSM 2903		Late Oligocene	Contamana CTA-61 (Chambira Fm.), Peru	Multiserial sbt 2-3	Boivin et al. (2019a)
			MUSM 2904		Late Oligocene	Contamana CTA-61 (Chambira Fm.), Peru	Multiserial sbt 2	Boivin et al. (2019a)
			MUSM 2905		Late Oligocene	Contamana CTA-61 (Chambira Fm.), Peru	Multiserial sbt 2	Boivin et al. (2019a)
			MUSM 2906		Late Oligocene	Contamana CTA-61 (Chambira Fm.), Peru	Multiserial sbt 2	Boivin et al. (2019a)
			MUSM 2907		Late Oligocene	Contamana CTA-61 (Chambira Fm.), Peru	Multiserial sbt 2	Boivin et al. (2019a)
			MUSM 3510		Late Eocene	Tarapoto/Baslayacu TAR-56 (lower mb. Pozo Fm.), Peru	Multiserial sbt 2	Assemat et al. (2019)
			MUSM 3509		Late Eocene	Tarapoto/Baslayacu TAR-56 (lower mb. Pozo Fm.), Peru	Multiserial sbt 1	Assemat et al. (2019)
			MUSM 3508		Late Eocene	Tarapoto/Baslayacu TAR-56 (lower mb. Pozo Fm.), Peru	Multiserial sbt 1	Assemat et al. (2019)
			MUSM 3518		Late Eocene	Tarapoto/Baslayacu TAR-55bis (lower mb. Pozo Fm.), Peru	Multiserial sbt 2	Assemat et al. (2019)
			MUSM 3517		Late Eocene	Tarapoto/Baslayacu TAR-55bis (lower mb. Pozo Fm.), Peru	Multiserial sbt 1-2	Assemat et al. (2019)
			MUSM 3516		Late Eocene	Tarapoto/Baslayacu TAR-55bis (lower mb. Pozo Fm.), Peru	Multiserial sbt 2	Assemat et al. (2019)
			MUSM 3513		Late Eocene	Tarapoto/Baslayacu TAR-55 (lower mb. Pozo Fm.), Peru	Multiserial sbt 2	Assemat et al. (2019)
			MUSM 3512		Late Eocene	Tarapoto/Baslayacu TAR-55 (lower mb. Pozo Fm.), Peru	Multiserial sbt 2	Assemat et al. (2019)
			MUSM 3511		Late Eocene	Tarapoto/Baslayacu TAR-55 (lower mb. Pozo Fm.), Peru	Multiserial sbt 1-2	Assemat et al. (2019)
			MUSM 3519		Late Eocene	Tarapoto/Juanjui TAR-45 (? Pozo Fm.), Peru	Multiserial sbt 1	Assemat et al. (2019)
			MUSM 3531		Late Eocene	Tarapoto/Juanjui TAR-47 (? Pozo Fm.), Peru	Multiserial sbt 2	Assemat et al. (2019)
			MUSM 3530		Late Eocene	Tarapoto/Juanjui TAR-47 (? Pozo Fm.), Peru	Multiserial sbt 2	Assemat et al. (2019)
			MUSM 3529		Late Eocene	Tarapoto/Juanjui TAR-47 (? Pozo Fm.), Peru	Multiserial sbt 2	Assemat et al. (2019)
			MUSM 3528		Late Eocene	Tarapoto/Juanjui TAR-47 (? Pozo Fm.), Peru	Multiserial sbt 1-2	Assemat et al. (2019)
			MUSM 3527		Late Eocene	Tarapoto/Juanjui TAR-47 (? Pozo Fm.), Peru	Multiserial sbt 2	Assemat et al. (2019)
			MUSM 3526		Late Eocene	Tarapoto/Juanjui TAR-47 (? Pozo Fm.), Peru	Multiserial sbt 2-3	Assemat et al. (2019)
			MUSM 3533		Latest Eocene/earliest Oligocene	Tarapoto/Juanjui TAR-49 (? Pozo Fm.), Peru	Multiserial sbt 2-3	Assemat et al. (2019)
			MUSM 3534		Latest Eocene/earliest Oligocene	Tarapoto/Juanjui TAR-49 (? Pozo Fm.), Peru	Multiserial sbt 2-3	Assemat et al. (2019)
			MUSM 3539		Latest Eocene/earliest Oligocene	Tarapoto/Juanjui TAR-50 (? Pozo Fm.), Peru	Multiserial sbt 2-3	Assemat et al. (2019)
			MUSM 3342		Earliest Oligocene	Tarapoto/Shapaja TAR-01 (upper mb. Pozo Fm.), Peru	Multiserial sbt 2	Boivin et al. (2019a)
			MUSM 3343		Earliest Oligocene	Tarapoto/Shapaja TAR-01 (upper mb. Pozo Fm.), Peru	Multiserial sbt (2)-3	Boivin et al. (2019a)
			MUSM 3344		Earliest Oligocene	Tarapoto/Shapaja TAR-01 (upper mb. Pozo Fm.), Peru	Multiserial sbt 1-2	Boivin et al. (2019a)
			MUSM 3345		Earliest Oligocene	Tarapoto/Shapaja TAR-01 (upper mb. Pozo Fm.), Peru	Multiserial sbt 2	Boivin et al. (2019a)
			MUSM 3346		Earliest Oligocene	Tarapoto/Shapaja TAR-01 (upper mb. Pozo Fm.), Peru	Multiserial sbt 3	Boivin et al. (2019a)
			MUSM 3347		Earliest Oligocene	Tarapoto/Shapaja TAR-01 (upper mb. Pozo Fm.), Peru	Multiserial sbt 2	Boivin et al. (2019a)
			MUSM 3348		Earliest Oligocene	Tarapoto/Shapaja TAR-01 (upper mb. Pozo Fm.), Peru	Multiserial sbt 2-3	Boivin et al. (2019a)
			MUSM 3349		Earliest Oligocene	Tarapoto/Shapaja TAR-01 (upper mb. Pozo Fm.), Peru	Multiserial sbt 3	Boivin et al. (2019a)
			MUSM 3350		Earliest Oligocene	Tarapoto/Shapaja TAR-01 (upper mb. Pozo Fm.), Peru	Multiserial sbt 2	Boivin et al. (2019a)
			MUSM 3351		Earliest Oligocene	Tarapoto/Shapaja TAR-01 (upper mb. Pozo Fm.), Peru	Multiserial sbt 2	Boivin et al. (2019a)
			MUSM 3352		Earliest Oligocene	Tarapoto/Shapaja TAR-01 (upper mb. Pozo Fm.), Peru	Multiserial sbt 3	Boivin et al. (2019a)
			MUSM 3353		Earliest Oligocene	Tarapoto/Shapaja TAR-01 (upper mb. Pozo Fm.), Peru	Multiserial sbt (1)-2	Boivin et al. (2019a)
Old World HYSTRICOGNATHI								
Stem hystricognaths								
	Phiocricetomyidae	Phiocricetomyinae		*"Protophiomys" tunisiensis*	Late middle Eocene	Djebel el Kébar, KEB-1, Tunisia	Multiserial sbt 1	Marivaux et al. (2014)
	"Protophiomyidae"	"Protophiomyinae"		*Protophiomys ?algeriensis*	Early late Eocene	Bir el Ater (BEA), Nementcha, Algeria	Multiserial sbt 2	Martin (1992, 1993)
	"Baluchimyidae"	"Baluchimyinae"		*Baluchimys krabiense*	Latest Eocene	Krabi, Bang Mark Pit, Peninsular Thailand	Multiserial sbt 1-2	Marivaux et al. (2000)
	"Bugtimyidae"	"Bugtimyinae"		cf. *Hodsahibia* sp.	Late early Oligocene	Zinda Pir Dome, Z-108 loc. (Chitarwata Fm.), Pakistan	Multiserial sbt 1-2	Martin (1995)
				Gen. et sp. indet. 1	Late early Oligocene	Zinda Pir Dome, Z-108 loc. (Chitarwata Fm.), Pakistan	Multiserial sbt 3	Martin (1995)
				Gen. et sp. indet. 2 (GSP 21557)	Early Oligocene	Bugti Hills, Y-GSP loc. 417 (Chitarwata Fm.), Pakistan	Multiserial sbt 1	Flynn et al. (1986)
				Gen. et sp. indet. 3 (GSP 21297)	Early Oligocene	Bugti Hills, Y-GSP loc. 417 (Chitarwata Fm.), Pakistan	Multiserial sbt 2	Martin (1992)
				Gen. et sp. indet. 4	Early Oligocene	Bugti Hills, DBC-2 (Chitarwata Fm.), Pakistan	Multiserial sbt 2–3	Marivaux (2000)
				Gen. et sp. indet. 5	Early Oligocene	Bugti Hills, DBC-2 (Chitarwata Fm.), Pakistan	Multiserial sbt 2	Marivaux (2000)
				Gen. et sp. indet. 6	Early Oligocene	Bugti Hills, DBC-2 (Chitarwata Fm.), Pakistan	Multiserial sbt 3	Marivaux (2000)
			(or diatomyid)	Gen. et sp. indet. 7	Early Oligocene	Bugti Hills, DBC-2 (Chitarwata Fm.), Pakistan	Multiserial sbt 3	Marivaux (2000)
				Gen. et sp. indet. 8	Early Oligocene	Bugti Hills, DBC-2 (Chitarwata Fm.), Pakistan	Multiserial sbt 3	Marivaux (2000)
	Tsaganomyidae			*Tsaganomys altaicus*	Early Oligocene	Tsagan Nor Basin (Hsanda Gol Fm.), Mongolia	Multiserial sbt 2	Martin (1992)
				Tsaganomys sp.	Early Oligocene	Tsagan Nor Basin (Hsanda Gol Fm.), Mongolia	Multiserial sbt 2	Martin (1992)
Hystricoidea ?	Gaudeamuridae			*Gaudeamus aegyptius*	Early Oligocene	Fayum, Quarry E (Jebel Quatrani Fm.), Egypt	Multiserial sbt 2	Martin (1992)
				Gaudeamus lavocati	Early Oligocene	Zallah, Loc. Z5R, Libya	Multiserial sbt 2	Martin in Coster et al. (2010)
Hystricoidea	Hystricidae			*Hystrix cristata*	Recent		Multiserial sbt 1	Martin (1992)
				Hystrix sivalensis	Pliocene	Bhandar, Punjab (Dhok Pathan Fm.), Pakistan	Multiserial sbt 2	Martin (1992)
				Atherurus africanus	Recent		Multiserial sbt 1	Martin (1992)
PHIOMORPHA								
Thryonomyoidea	Phiomyidae			*Phiomys andrewsi*	Early Oligocene	Fayum, Quarry E (Jebel Quatrani Fm.), Egypt	Multiserial sbt 2	Martin (1992)
	"Metaphiomyidae"	"Metaphiomyinae"		*Turkanamys hexalophus*	Early late Oligocene	Lokone Hill (LOK 13), Turkana Basin, Kenya	Multiserial sbt 2	Marivaux et al. (2012)
	Thryonomyidae			*Metaphiomys schaubi*	Early Oligocene	Fayum, Quarry E (Jebel Quatrani Fm.), Egypt	Multiserial sbt 3	Martin (1992)
				Paraphiomys pigotti	Early Miocene	Rusinga, Kenya	Multiserial sbt 3	Martin (1992)
				Thryonomys swindermnus	Recent		Multiserial sbt 2-3	Martin (1992)
	Diamantomyidae			*Diamantomys luederitzi*	Early Miocene	Songhor, Kenya	Multiserial sbt 1	Martin (1992)
	Petromuridae			*Petromus typicus*	Recent		Multiserial sbt 3	Martin (1992)
	Bathyergidae			*Bathyergus suillus*	Recent		Multiserial sbt 2-3	Martin (1992)

PARVORDER and Superfamily	Family	Subfamily	Species / Specimen number	Taxonomic remark*	Age	Locality (Loc.) and/or Formation (Fm.) for extinct species	Multiserial subtype (sbt)	References regarding the enamel microstructure
			Cryptomys hottentotus		Recent		Multiserial sbt 2-3	Martin (1992)
			Cryptomys mechowi		Recent		Multiserial sbt 2-3	Martin (1992)
			Georychus capensis		Recent		Multiserial sbt 2-3	Martin (1992)
			Heliophobius argenteocinereus		Recent		Multiserial sbt 2-3	Martin (1992)
			Heterocephalus glaber		Recent		Multiserial sbt 2-3	Martin (1992)
			Heterocephalus jaegeri		Pleistocene	Olduvai Bed. I, Tanzania	Multiserial sbt 2-3	Martin (1992)
			DAK-Pto-037		Earliest Oligocene	Dakhla-Porto Rico DAK-Pto C2 (Upper Samlat Fm.), Morocco	Multiserial sbt 2	Marivaux et al. (2019)
			DAK-Pto-042		Earliest Oligocene	Dakhla-Porto Rico DAK-Pto C2 (Upper Samlat Fm.), Morocco	Multiserial sbt 2	Marivaux et al. (2019)
			DAK-Pto-039		Earliest Oligocene	Dakhla-Porto Rico DAK-Pto C2 (Upper Samlat Fm.), Morocco	Multiserial sbt 2	Marivaux et al. (2019)
			DAK-Pto-041		Earliest Oligocene	Dakhla-Porto Rico DAK-Pto C2 (Upper Samlat Fm.), Morocco	Multiserial sbt 2	Marivaux et al. (2019)
			DAK-Pto-044		Earliest Oligocene	Dakhla-Porto Rico DAK-Pto C2 (Upper Samlat Fm.), Morocco	Multiserial sbt 2	Marivaux et al. (2019)
			DAK-Pto-038		Earliest Oligocene	Dakhla-Porto Rico DAK-Pto C2 (Upper Samlat Fm.), Morocco	Multiserial sbt (1)-2	Marivaux et al. (2019)
			DAK-Pto-040		Earliest Oligocene	Dakhla-Porto Rico DAK-Pto C2 (Upper Samlat Fm.), Morocco	Multiserial sbt 2	Marivaux et al. (2019)
			DAK-Pto-047		Earliest Oligocene	Dakhla-Porto Rico DAK-Pto C2 (Upper Samlat Fm.), Morocco	Multiserial sbt 2	Marivaux et al. (2019)
			DAK-Pto-045		Earliest Oligocene	Dakhla-Porto Rico DAK-Pto C2 (Upper Samlat Fm.), Morocco	Multiserial sbt 2	Marivaux et al. (2019)
			DAK-Pto-046		Earliest Oligocene	Dakhla-Porto Rico DAK-Pto C2 (Upper Samlat Fm.), Morocco	Multiserial sbt 2	Marivaux et al. (2019)
			DAK-Pto-048		Earliest Oligocene	Dakhla-Porto Rico DAK-Pto C2 (Upper Samlat Fm.), Morocco	Multiserial sbt 2	Marivaux et al. (2019)
			DAK-Pto-049		Earliest Oligocene	Dakhla-Porto Rico DAK-Pto C2 (Upper Samlat Fm.), Morocco	Multiserial sbt 2	Marivaux et al. (2019)
			DAK-Pto-050		Earliest Oligocene	Dakhla-Porto Rico DAK-Pto C2 (Upper Samlat Fm.), Morocco	Multiserial sbt (1)-2	Marivaux et al. (2019)
			DAK-Pto-051		Earliest Oligocene	Dakhla-Porto Rico DAK-Pto C2 (Upper Samlat Fm.), Morocco	Multiserial sbt 2	Marivaux et al. (2019)
			DAK-Arg-072		Earliest Oligocene	Dakhla-El Argoub DAK-Arg C2 (Upper Samlat Fm.), Morocco	Multiserial sbt 2	Marivaux et al. (2019)
			DAK-Arg-074		Earliest Oligocene	Dakhla-El Argoub DAK-Arg C2 (Upper Samlat Fm.), Morocco	Multiserial sbt 2	Marivaux et al. (2019)
			DAK-Arg-075		Earliest Oligocene	Dakhla-El Argoub DAK-Arg C2 (Upper Samlat Fm.), Morocco	Multiserial sbt 2	Marivaux et al. (2019)
			DAK-Arg-076		Earliest Oligocene	Dakhla-El Argoub DAK-Arg C2 (Upper Samlat Fm.), Morocco	Multiserial sbt 2	Marivaux et al. (2019)
			DAK-Arg-085		Earliest Oligocene	Dakhla-El Argoub DAK-Arg C2 (Upper Samlat Fm.), Morocco	Multiserial sbt 2	Marivaux et al. (2019)
			DAK-Arg-086		Earliest Oligocene	Dakhla-El Argoub DAK-Arg C2 (Upper Samlat Fm.), Morocco	Multiserial sbt 2	Marivaux et al. (2019)
			DAK-Arg-078		Earliest Oligocene	Dakhla-El Argoub DAK-Arg C2 (Upper Samlat Fm.), Morocco	Multiserial sbt 2	Marivaux et al. (2019)
			DAK-Arg-080		Earliest Oligocene	Dakhla-El Argoub DAK-Arg C2 (Upper Samlat Fm.), Morocco	Multiserial sbt 2	Marivaux et al. (2019)
			DAK-Arg-077		Earliest Oligocene	Dakhla-El Argoub DAK-Arg C2 (Upper Samlat Fm.), Morocco	Multiserial sbt 2	Marivaux et al. (2019)
			DAK-Arg-079		Earliest Oligocene	Dakhla-El Argoub DAK-Arg C2 (Upper Samlat Fm.), Morocco	Multiserial sbt 2	Marivaux et al. (2019)
			DAK-Arg-081		Earliest Oligocene	Dakhla-El Argoub DAK-Arg C2 (Upper Samlat Fm.), Morocco	Multiserial sbt 2	Marivaux et al. (2019)
			DAK-Arg-082		Earliest Oligocene	Dakhla-El Argoub DAK-Arg C2 (Upper Samlat Fm.), Morocco	Multiserial sbt 2	Marivaux et al. (2019)
			DAK-Arg-083		Earliest Oligocene	Dakhla-El Argoub DAK-Arg C2 (Upper Samlat Fm.), Morocco	Multiserial sbt 2	Marivaux et al. (2019)
			DAK-Arg-084		Earliest Oligocene	Dakhla-El Argoub DAK-Arg C2 (Upper Samlat Fm.), Morocco	Multiserial sbt 2	Marivaux et al. (2019)
Afro-Asian 'Ctenodactyloidea'								
	Cocomyidae		*Cocomys lingchaensis*		Early Eocene	Hengdong County, Hanan Province, China	Pauciserial	Martin (1992, 1995)
			Cocomys sp.		Early Eocene	NC	Pauciserial	Martin (2007)
			Alaymys ctenodactylus		Early Eocene	Andarak 2, Kyrgyzstan	Pauciserial	Martin (2007)
	Chappatimyidae		cf. *Birbalomys* sp.		Middle Eocene	Metka, Kalakot, India	Pauciserial	Martin (1992, 1995)
			Gen. et sp. indet.		Middle Eocene	Kala Chitta Range (Jhalar section), Pakistan	Pauciserial	Martin (1992, 1995)
	Yuomyidae		*Advenimus ulungurus*		Early Eocene	Ulungur River, Junggae Basin, Xinjiang Uygur, China	Pauciserial	Meng et al. (2001)
			cf. *Advenimus* sp.		Middle Eocene	Ulan Shiiah beds, Mongolia	Pauciserial	Martin (2007)
			Petrokozlovia notos		Middle Eocene	Khaichin Ula II, Mongolia	Pauciserial	Martin (2007)
			Petrokozlovia cf. *notos*		Early Eocene	Andarak 2, Kyrgyzstan	Pauciserial	Martin (2007)
			Yuomys sp.		Middle Eocene	"Tomb Ridge", Xiangshan Fm., Yunnan, China	Pauciserial	Martin (2007)
	Tanquammyidae		*Tsagamys subitus*		Early Eocene	Tsagan Kushu, Mongolia	Pauciserial	Martin (1993)
			cf. *Tanquammys* sp.		Middle Eocene	Khaychin Ula II, Mongolia	Multiserial sbt 1	Martin (1993, 1995)
	?		*Euboromys* sp. indet.		Middle Eocene	Khaychin Ula II, Mongolia	Pauci- to multiserial	Martin (1993)
	Ctenodactylidae		*Karakoromys decessus*		Early Oligocene	Tsagan Nor Basin (Hsanda Gol Fm.), Mongolia	Multiserial sbt 2	Martin (2007)
			Tataromys plicidens		Early Oligocene	Tsagan Nor Basin (Hsanda Gol Fm.), Mongolia	Multiserial sbt 2	Martin (2007)
			Yindirtemys deflexus		Early Oligocene	Tsagan Nor Basin (Hsanda Gol Fm.), Mongolia	Multiserial sbt 2	Martin (2007)
			Yindirtemys suni		Early Oligocene	Tsagan Nor Basin (Hsanda Gol Fm.), Mongolia	Multiserial sbt 2	Martin (2007)
			Leptotataromys sp.		Late Oligocene	Ulantatal (UTL 1), Inner Mongolia	Multiserial sbt 2	Martin (1992, 1995)
			Sayimys sivalensis		Middle Miocene	H-G3 (lower Manchar Fm.), Sind, Pakistan	Multiserial sbt 3	Martin (1992, 1995)
			Sardomys dawsonae		Late Miocene	Oschiri, Sardinia	Multiserial sbt 3	Martin (1992, 1995)
			Africanomys minor		Late Miocene	Pataniak 6, Morocco	Multiserial sbt 3	Martin (1992, 1995)
			Pellegrinia panormensis		Pleistocene	Monte Pellegrino, Sicily	Multiserial sbt 3	Martin (1992, 1995)
			Ctenodoctylus gundi		Recent		Multiserial sbt 3	Martin (1992, 1995)
			Felovia vae		Recent		Multiserial sbt 3	Martin (1992, 1995)
			Massoutiera mzabi		Recent		Multiserial sbt 3	Martin (1992, 1995)
	Diatomyidae		*Fallomus ladakhensis*		Late Oligocene	Cha Prong pit of Nong Ya Plong coal mine, Phetchaburi Province, Thailand	Multiserial sbt 2–3	Marivaux et al. (2004)
			cf. *Diatomys liensis*		Middle Miocene	Mae Long, Li Basin, Thailand	Multiserial sbt 2	Martin (1995)
			Laonastes aenigmamus		Recent	Khammouan Province, Laos	Multiserial sbt 3	Marivaux in Dawson et al. (2006)

*Corresponds to the extant and extinct taxa, for which synonymy was made, based on Woods (1993), Candela (2000), Candela and Nasif (2006), Vucetich et al. (2010), Patton et al. (2015), Rasia (2016), and Rasia and Candela (2016)

The systematics derives from Upham and patterson (2015), Boivin et al. (2019b), and Courcelle et al. (2019) (and cited references therein)

References

Arnal M, Kramarz AG, Vucetich MG, Vieytes EC (2014) A new early Miocene octodontoid rodent (Hystricognathi, Caviomorpha) from Patagonia (Argentina) and a reassessment of the early evolution of Octodontoidea. J Vert Paleontol 34:397-406.

Assemat A, Boivin M, Marivaux L et al (2019) Restes inédits de rongeurs caviomorphes du Paléogène de la région de Juanjui (Amazonie péruvienne) : systématique, implications macro-évolutives et biostratigraphiques. Geodiversitas 41:699-730.

Barbière F, Marivaux L (2015) Phylogeny and evolutionary history of hystricognathous rodents from the Old World during the Tertiary: new insights into the emergence of modern "phiomorph" families. In: Cox FG, Hautier L (eds) Evolution of the Rodents: Advances in Phylogenetics, Functional Morphology and Development. Cambridge University Press, Cambridge, pp 87-138.

Boivin M, Marivaux L, Salas-Gismondi R, Vieytes EC, Antoine P-O (2019a) Incisor enamel microstructure of Paleogene caviomorph rodents from Contamana and Shapaja (Peruvian Amazonia). J Mamm Evol 26:389-406.

Boivin M, Marivaux L, Antoine P-O (2019b) L'apport du registre paléogène d'Amazonie sur la diversification initiale des Caviomorpha (Hystricognathi, Rodentia) : implications phylogénétiques, macroévolutives et paléobiogéographiques. Geodiversitas 41:143-245.

Coster P, Benammi M, Lazzari V et al (2010) *Gaudeamus lavocati* sp. nov. (Rodentia, Hystricognathi) from the early Oligocene of Zallah, Libya: first African caviomorph? Naturwissenschaften 97:697-706.

Dawson MR, Marivaux L, Li C-K, Beard KC, Métais G (2006) *Laonastes* and the "lazarus effect" in Recent mammals. Science 311:1456-1458.

Flynn LJ, Jacobs LL, Cheema IU (1986) Baluchimyinae, a new ctenodactyloid rodent subfamily from the Miocene of Baluchistan. Am Mus Novitates 2841:1-58.

Marivaux L. (2000) Les rongeurs de l'Oligocène des Collines Bugti (Balouchistan, Pakistan) : nouvelles données sur la phylogénie des Rongeurs paléogènes, implications biochronologiques et paléobiogéographiques. PhD, Université des Sciences et Techniques du Languedoc, Montpellier.

Marivaux L, Benammi M, Ducrocq S, Jaeger J-J, Chaimanee Y (2000) A new baluchimyine rodent from the Late Eocene of the Krabi Basin (Thailand): paleobiogeographic and biochronologic implications. C R Acad Sci, Paris 331:427-433.

Marivaux L, Chaimanee Y, Yamee C, Srisuk P, Jaeger J-J (2004) Discovery of *Fallomus ladakhensis* Nanda & Sahni, 1998 (Rodentia, Diatomyidae) in the lignites of Nong Ya Plong (Phetchaburi Province, Thailand): systematic, biochronologic and paleoenvironmental implications. Geodiversitas 26:493-507.

Marivaux L, Lihoreau F, Manthi KF, Ducrocq R (2012) A new basal phiomorph (Rodentia, Hystricognathi) from the Late Oligocene of Lokone (Turkana Basin, Kenya). J Vert Paleontol 32:646-657.

Marivaux L, Essid EM, Marzougui W, Khayati Ammar H, Adnet S, Marandat B, Merzeraud G, Tabuce R, Vianey-Liaud M (2014) A new and primitive species of *Protophiomys* (Rodentia, Hystricognathi) from the late middle Eocene of Djebel el Kébar, Central Tunisia. Palaeovertebrata 38:1-17.

Marivaux L, Boivin M, Adnet S, Benammi M, Tabuce R, Benammi M (2019) Incisor enamel microstructure of hystricognathous and anomaluroid rodents from the earliest Oligocene of Dakhla, Atlantic Sahara (Morocco). J Mamm Evol 26:373-388.

Marivaux L, Vélez-Juarbe J, Merzeraud G et al (2020) Early Oligocene chinchilloid caviomorphs from Puerto Rico and the initial rodent colonization of the West Indies. Proc Roy Soc B 287:20192806.

Martin T (1992) Schmelzmikrostruktur in den inzisiven alt-und neuweltlicher hystricognather nagetiere. Palaeovertebrata Mém. extra.:1-168.

Martin T (1993) Early rodent incisor enamel evolution: phylogenetic implications. J Mamm Evol 1:227-254.

Martin T (1994a) On the systematic position of *Chaetomys subspinosus* (Rodentia: Caviomorpha) based on evidence from the incisor enamel microstructure. J Mamm Evol 2:117-131.

Martin T (1994b) African origin of caviomorph rodents is indicated by incisor enamel microstructure. Paleobiology 20:5-13.

Martin T (1995) Incisor enamel microstructure and phylogenetic interrelationships of Pedetidae and Ctenodactyloidea (Rodentia). Berliner Geowiss Abh 16:693-707.

Martin T (1997) Incisor enamel microstructure and systematics in rodents. In: Koenigswald Wv, Sander PM (eds) Tooth Enamel Microstructure. Balkema, Rotterdam, pp 163-175.

Martin T (2004) Incisor enamel microstructure of South America's earliest rodents: implications for caviomorph origin and diversification. In: Campbell KE (ed) The Paleogene Mammalian Fauna of Santa Rosa, Amazonian Peru. Natural History Museum of Los Angeles County, Los Angeles, pp 131-140.

Martin T (2005) Incisor schmelzmuster diversity in South America's oldest rodent fauna and early caviomorph history. J Mamm Evol 12:405-417.

Martin T (2007) Incisor enamel microstructure and the concept of Sciuravida. In: Beard KC, Luo Z-X (eds) Mammalian Paleontology on a Global Stage: Papers in Honor of Mary R Dawson. Bull Carnegie Mus Nat Hist, Pittsburgh, pp 127-140.

Meng J, Wu W-Y, Ye J (2001) A new species of *Advenimus* (Rodentia, Mammalia) from the Eocene of Northern Junggar basin of Xinjiang, China. Vertebr PalAsiatica 39:186-196.

Morgan CC, Verzi DH, Olivares AI, Vieytes EC (2017) Craniodental and forelimb specializations for digging in the South American subterranean rodent *Ctenomys* (Hystricomorpha, Ctenomyidae). Mamm Biol 87:118-124.

Vélez-Juarbe J, Martin T, MacPhee RDE, Ortega-Ariza D (2014) The earliest Caribbean rodents: Oligocene caviomorphs from Puerto Rico. J Vert Paleontol 34:157-163.

Vieytes EC. (2003) Microestructura del esmalte de roedores Hystricognathi sudamericanos fósiles y vivientes: significado morfofuncional y filogenético. PhD, Universidad Nacional de La Plata, La Plata.

Vieytes EC, Morgan CC, Verzi DH (2007) Adaptive diversity of incisor enamel microstructure in South American burrowing rodents (family Ctenomyidae, Caviomorpha). J Anat 211:296-302.

Vucetich MG, Vieytes EC (2006) A middle Miocene primitive octodontoid rodent and its bearing on the early evolutionary history of the Octodontoidea. Palaeontogr Abt A 277:81–91.

Vucetich MG, Kramarz AG, Candela AM (2010) Colhuehuapian rodents from Gran Barranca and other Patagonian localities: the state of the art. In: Madden RH, Carlini AA, Vucetich MG, Kay RF (eds) The Paleontology of Gran Barranca: Evolution and Environmental Change through the Middle Cenozoic of Patagonia. Cambridge University Press, New York, pp 206-219.

Online Resource 1_Summary of incisor enamel among Ctenohystrica

Vucetich MG, Arnal M, Deschamps CM, Pérez ME, Vieytes EC (2015) A brief history of caviomorph rodents as told by the fossil record. In: Vassallo AI, Antenucci D (eds) Biology of Caviomorph Rodents: Diversity and Evolution. SAREM Series A, Buenos Aires, pp 11-62.